Received: 14 March 2022 | Revised: 12 June 2022 | Accepted: 15 June 2022

DOI: 10.1111/mpp.13244

Molecular Plant Pathology WILEY

ORIGINAL ARTICLE

The integration host factor regulates multiple virulence pathways in bacterial pathogen *Dickeya zeae* MS2

Shanshan Chen | Ming Hu | Anqun Hu | Yang Xue | Si Wang | Fan Liu | Chuhao Li | Xiaofan Zhou | Jianuan Zhou

Guangdong Province Key Laboratory of Microbial Signals and Disease Control, Integrative Microbiology Research Center, South China Agricultural University, Guangzhou, China

Correspondence
Jianuan Zhou, Guangdong Province Key Laboratory of Microbial Signals and Disease Control, Integrative Microbiology Research Center, South China Agricultural University, Guangzhou 510642, China.
Email: jianuanzhou@scau.edu.cn

Funding information
China Scholarship Council Fellowship Program Grant, Grant/Award Number: 202108440367; Guangzhou Basic Research Program, Grant/Award Number: 202102080613; Key-Area Research and Development Program of Guangdong Province, Grant/Award Number: 2020B0202090001 and 2018B020205003; National Natural Science Foundation of China, Grant/Award Number: 31972230; Natural Science Foundation of Guangdong Province, Grant/Award Number: 2020A1515011534

Abstract

Dickeya zeae is an aggressive bacterial phytopathogen that infects a wide range of host plants. It has been reported that integration host factor (IHF), a nucleoid-associated protein consisting of IHFα and IHFβ subunits, regulates gene expression by influencing nucleoid structure and DNA bending. To define the role of IHF in the pathogenesis of *D. zeae* MS2, we deleted either and both of the IHF subunit encoding genes *ihfA* and *ihfB*, which significantly reduced the production of cell wall-degrading enzymes (CWDEs), an unknown novel phytotoxin and the virulence factor-modulating (VFM) quorum-sensing (QS) signal, cell motility, biofilm formation, and thereafter the infection ability towards both potato slices and banana seedlings. To characterize the regulatory pathways of IHF protein associated with virulence, IHF binding sites (consensus sequence 5′-WATCAANNNNTTR-3′) were predicted and 272 binding sites were found throughout the genome. The expression of 110 tested genes was affected by IHF. Electrophoretic mobility shift assay (EMSA) showed direct interaction of IhfA protein with the promoters of *vfmE*, *speA*, *pipR*, *fis*, *slyA*, *prtD*, *hrpL*, *hecB*, *hcp*, *indA*, *hdaA*, *flhD*, *pilT*, *gcpJ*, *arcA*, *arcB*, and *lysR*. This study clarified the contribution of IHF in the pathogenic process of *D. zeae* by controlling the production of VFM and putrescine QS signals, phytotoxin, and indigoidine, the *luxR*-solo system, Fis, SlyA, and FlhD transcriptional regulators, and secretion systems from type I to type VI. Characterization of the regulatory networks of IHF in *D. zeae* provides a target for prevention and control of plant soft rot disease.

KEYWORDS
cell motility, cell wall-degrading enzymes, *Dickeya zeae*, DNA binding, integration host factor, transcriptional regulator, virulence

Shanshan Chen and Ming Hu contributed equally to this work.

1 | INTRODUCTION

Dickeya zeae, formerly named *Erwinia chrysanthemi* pv. *zeae*, is responsible for widespread outbreaks of banana bacterial soft rot disease (Samson et al., 2005; Zhang et al., 2013). The disease develops upwards from the base of the pseudostem to the growing point and causes soft rot in plant tissues with symptoms of leaf wilting and yellowing (Lin et al., 2010; Zhang et al., 2014). *D. zeae* strains isolated from different hosts, or even the same host species, have different degrees of virulence (Hu et al., 2018). The pathogen uses complex pathogenic mechanisms, mainly arising from the diversity of the virulence factors and pathogenic regulatory networks. Currently, four classes of pathogenic regulatory factors have been unveiled in *D. zeae*: a quorum-sensing (QS) system, cyclic-di GMP (c-di-GMP) signalling, two-component signal transduction systems (TCS), and transcription factors (TF) (Chen et al., 2016; Hommais et al., 2008; Lv et al., 2019; Reverchon et al., 1998). These regulatory factors coordinate to modulate pathogen virulence when induced by a variety of environmental factors.

Nucleoid-associated proteins (NAPs), which are chromosome-organizing factors, affect the transcriptional landscape of bacterial cells (Dey et al., 2017). Integration host factor (IHF), which is composed of two subunits IHFα and IHFβ, is a small heterodimer of NAPs (Reverchon et al., 2021). It can recognize specific DNA sequences and bind to the small groove of the DNA to form an IHF–DNA complex, resulting in DNA helix reversals over short distances (Rice et al., 1996; Yang & Nash, 1989). The earliest functional studies of IHF mainly focused on phages. IHF is able to specifically interact with phage attachment sites (*attP*) to regulate the expression of phage λ (Craig & Nash, 1984; Richet et al., 1986). IHF to positively regulates the early and repressor transcription of phage Mu by a type of binding site dependence (van Rijn et al., 1988). Genetic and biochemical studies have shown that IHF is involved in physiological processes of *Escherichia coli*, in which a conserved sequence of IHF binding sites in λ phage *attP* is also found within functional regions (Craig & Nash, 1984; Friedman, 1988). In *E. coli*, IHF binding to DNA depends on the consensus sequence 5′-WATCAANNNNTTR-3′(where W = A or T, N = any base, and R = A or G) (Craig & Nash, 1984; Yang & Nash, 1989). This consensus sequence is useful for predicting potential sites for IHF binding to DNA from other pathogenic bacteria. In *Vibrio cholerae* and *Vibrio fluvialis*, VgrG/TssI and its downstream effector and immune genes act as the tip component of the type VI secretion system (T6SS), and are positively regulated by the quorum-sensing (QS) regulator HapR and the global regulator IHF. IHF appears to be much more activated than HapR, suggesting that IHF may be a major regulator of the *vgrG* operon (Zhang et al., 2021). IHF activates the transcription of GbdR, a specific regulator of choline metabolism in *Pseudomonas aeruginosa* (German Sanchez et al., 2017). IHF also significantly regulates the expression of RpoN-dependent *hrpL* and other type III secretion system (T3SS) genes, and is essential for *Erwinia amylovora* virulence. In addition, it regulates swimming motility through activation of sRNA *rsmB* expression (Lee & Zhao, 2016). In *Pseudomonas putida*, IHF promotes the frequency of homologous recombination and point mutations (Mikkel et al., 2020). Notably, Fis has been identified as a global regulator that has complex interactions with IHF, as reflected in the ability of both to identify consensus *cis*-elements and consensus binding sites (Oliveira Monteiro et al., 2020). Recently, it was found that IhfA is able to bind to the promoter region of a diguanylate cyclase-encoding gene to alter the c-di-GMP expression level and regulate pathogenicity as well as other physiological functions in *Dickeya oryzae* (Chen et al., 2019).

Numerous studies have confirmed the important role of IHF in bacteria, including affecting gene expression, controlling cell metabolism, and inducing DNA bending (Prieto et al., 2012; Reverchon et al., 2021; van Rijsewijk et al., 2011). However, the regulatory mechanism of IHF in *D. zeae* is unclear, and in particular how IHF directly interacts with downstream genes associated with virulence is still unknown. This study aims to clarify the specific pathways directly regulated by IHF to affect the virulence of *D. zeae*.

2 | RESULTS

2.1 | Deletion of IHF slightly affects the growth of *D. zeae* MS2

To study the role of IHF in the pathogenicity of *D. zeae* MS2, single knockout mutants, Δ*ihfA* and Δ*ihfB*, and a double knockout mutant, Δ*ihfAB*, were first generated by homologous recombination. Subsequently, complemented strains of Δ*ihfA* and Δ*ihfB* were constructed by in trans expression of genes into the corresponding mutants using a low-copy expression vector pLAFR3, respectively named as Δ*ihfA*::*ihfA* and Δ*ihfB*::*ihfB*. To compare the growth rate of MS2 and its derivatives, optical density values at 600 nm within 48 h were recorded using Bioscreen C. As shown in Figure S1, Δ*ihfA*, Δ*ihfB*, and Δ*ihfAB* grew slightly slower than MS2 and the complemented strains. However, the growth of the complemented strains was greater than that of MS2 at 12–48 h postincubation. These results showed that the deletion of IHF slightly affects the growth of *D. zeae* MS2, which is similar to the situation in *Dickeya dadantii* 3937 and *D. oryzae* EC1 (Chen et al., 2019; Reverchon et al., 2021).

2.2 | IHF is a global transcriptional regulator modulating the expression of over 100 genes in *D. zeae* MS2

Because IHF is known to modulate multiple phenotypes associated with virulence in many pathogenic bacteria, to identify the regulatory pathways of IHF associated with virulence in *D. zeae* we first searched for the IHF binding motif (5′-WATCAANNNNTTR-3′) throughout the MS2 genome. The results revealed a total of 272 candidates with IHF binding sites in the promoter regions of

coding sequences (CDS) in the MS2 genome (Table S1). To verify whether the promoters interact with IHF, reverse transcription-quantitative PCR (RT-qPCR) was performed to analyse the expression of the genes downstream of 128 randomly selected promoters from the 272 candidates in the *ihf* mutants in comparison to the wild type (Table 1). According to the RT-qPCR results, the expression of 110 genes was significantly regulated by IHF, 105 positively and 5 negatively (Table 1). The predicted functions of the regulated genes indicated that IHF could regulate a variety of physiological, stress resistance, and pathogenic phenotypes of *D. zeae* MS2, for instance metabolic processes including the transport of nutrients, cations, and amino acids, signal transduction, secretion systems, production of secondary metabolites and cell wall-degrading enzymes (CWDEs), and capsular polysaccharide synthesis (Table 1).

2.3 | IHF positively regulates the virulence factor-modulating and putrescine QS systems

The virulence of *Dickeya* spp. is controlled by highly sophisticated regulatory networks, a crucial one of which is the regulation by QS systems including the N-acylhomoserine lactone (AHL) system encoded by *expIR* (Feng et al., 2019; Hussain et al., 2008), the virulence factor-modulating (VFM) system encoded by the *vfm* gene cluster (Lv et al., 2019; Nasser et al., 2013), and the putrescine system, encoded by *speA* and *speC* (Liu et al., 2022; Shi et al., 2019). Furthermore, a *luxR*-solo system has also been characterized in *D. zeae* MS2, which regulates the activity of proline iminopeptidase PipA and contributes to the virulence of MS2 by an unknown mechanism (Feng et al., 2019). To determine whether IHF regulates QS systems in *D. zeae* MS2, RT-qPCR analysis of the expression of specific QS systems was performed. The results showed that deletion of *ihfA*, *ihfB*, and *ihfAB* significantly decreased the expression of *vfmE*, *speA*, *speC*, *pipR*, and *pipA*, but not the expression of *expI* and *expR* (Table 1). To determine whether IHF could directly interact with these genes, an electrophoretic mobility shift assay (EMSA) was performed to test the binding ability of IHF to their promoters containing the IHF motif. The results showed that 2.5 μM of IhfA protein could bind to the promoter regions of *vfmE*, *speA*, and *pipR* but not *speC* (Figure 1). In addition, the production of AHL and VFM QS signals was also measured using the biosensors previously described (Hussain et al., 2008; Lv et al., 2019). The results indicated that deletion of the IHF proteins did not affect the production of the AHL signal (Figure 2a), but dramatically blocked the production of the VFM signal (Figure 2b).

2.4 | IHF positively regulates the production of CWDEs via multiple regulatory pathways

CWDEs, including pectinases, cellulases, and proteases that degrade the structure of host plant cells, are important pathogenicity factors in *Dickeya* spp. and cause soft rot symptoms (Hugouvieux-Cotte-Pattat et al., 1996). Semiquantitative measurement of the enzymatic activities showed that deletion of *ihf* significantly reduced the activities of cellulases, pectate lyases, polygalacturonases, and proteases (Figure 3a).

In-depth study of virulence factors in *Dickeya* pathogens has revealed multiple complex regulatory pathways controlling the production of CWDEs. The first one is the VFM QS system regulating the generation of CWDEs (Lv et al., 2019; Nasser et al., 2013). Because IhfA directly binds to the promoter of *vfmE* (Figure 1), the decreased production of the VFM signal (Figure 2b) is one of the causes of the reduced production of CWDEs in the *ihf* mutants. Many transcriptional regulators are known to participate in the regulation of CWDE production, such as PecS, PecT, H-NS, SlyA, Fis, and KdgR (Hommais et al., 2008; Lv et al., 2018; Nasser & Reverchon, 2002; Rodionov et al., 2004; Zhou et al., 2016). IHF significantly regulated the expression of *fis*, *slyA*, *pecT*, and two H-NS genes *hnsA* and *hnsB* (Table 1). The EMSA results also confirmed the direct interaction of IhfA with *fis* and *slyA* promoters (Figure 1).

2.5 | IHF positively regulates the expression of type I to type VI secretion systems

Secretion systems, such as the type I secretion system (T1SS) and the type II secretion system (T2SS), responsible for the secretion of CWDEs, might be influenced by IHF proteins. Therefore, the expression of the genes related to secretion systems that harboured the predicted IHF binding motif was tested in the *ihf* mutants. Among the regulated genes, *prtD* expression was significantly reduced (2.34–3.27 $\log_2$ fold change) in the Δ *ihfA*, Δ*ihfB*, and Δ *ihfAB* mutants compared with that in wild-type MS2 (Table 1). The EMSA results also confirmed the direct interaction of IhfA with the *prtD* promoter (Figure 1). *prtD* is the first gene of the T1SS operon *prtDEF*, responsible for the secretion of proteases (Lory, 1998; Palacios et al., 2001). The reduced expression of *prtD* in the mutants probably results in less secretion of proteases and smaller protease degradative halos (Figure 3a). The expression of the *gspC* gene, encoding the inner membrane protein GspC of T2SS, decreased by 2.45–4.06 $\log_2$ fold change in the *ihf* mutants (Table 1). The T2SS is devoted to the secretion of most extracellular pectinases and cellulases that promote host invasion (Login et al., 2010; Wang et al., 2012), reasonably explaining the reasons for the decreased enzymatic activities of pectinases and cellulases of the *ihf* mutants (Figure 3a). The lack of binding to the *gspC* probe suggests an indirect regulation of IHF on T2SS expression (Figure 1).

The type III secretion system (T3SS) encoded by the *dsp/hrp/hrc* gene clusters in *D. zeae* MS2 has been studied recently and also contributes to the host range and virulence of *D. zeae* (Hu et al., 2022). In the T3SS, HrpL is the master regulator controlling the expression of the whole system and the effectors (T3SEs) in *Dickeya*, *Erwinia*, and

TABLE 1 Gene candidates harbouring the IHF binding motif predicted in *Dickeya zeae* MS2 genome and their expression in *ihfA* and *ihfB* mutants in comparison to the wild type

Function category	Gene	Locus (C1O30_)	Product	Binding site (5′-WATCAANNNNTTR-3′)[a]	Position from start codon	Log$_2$ fold change of gene expression[b]					
						Δ*ihfA*		Δ*ihfB*		Δ*ihfAB*	
Signal transduction	*vfmE*	RS00505	AraC family transcriptional regulator	AATCAACCACTGA	−99 to −73	−3.01 ± 0.16	↓	−5.01 ± 0.09	↓	−2.61 ± 0.13	↓
	expR	RS00610	LuxR family transcriptional regulator	AAT*T*AATAGACTA	−234 to −208	0.01 ± 0.05	–	−0.10 ± 0.09	–	−0.18 ± 0.07	–
	expI	RS00615	Acyl-homoserine-lactone synthase	AATCAAGCAATAA	−100 to −74	0.08 ± 0.14	–	−0.29 ± 0.27	–	−0.56 ± 0.14	–
	/	RS05855	TonB-dependent siderophore receptor	TATCAACAATTTT	−69 to −43	−4.32 ± 0.23	↓	−4.01 ± 0.06	↓	−4.22 ± 0.41	↓
	citA	RS09785	Sensor histidine kinase regulating citrate/malate metabolism	AATCAAATGATTG	−309 to −283	0.05 ± 0.08	–	−3.11 ± 0.13	↓	−1.49 ± 0.16	↓
	narX	RS11960	Nitrate/nitrite two-component system sensor histidine kinase NarX	CATCAACAGCTTG	−377 to −351	−1.64 ± 0.14	↓	−0.74 ± 0.30	–	−0.91 ± 0.10	–
	narL	RS11965	Two-component system response regulator NarL	AATCAACGGCTCG	−390 to −364	−3.15 ± 0.14	↓	−0.66 ± 0.12	–	−1.73 ± 0.19	↓
	pipR	RS14530	LuxR-solo transcriptional regulator	TATCAACGCGGTA	547 to −521	−4.13 ± 0.62	↓	−4.99 ± 0.53	↓	−3.42 ± 0.44	↓
	pipA	RS14535	Proline iminopeptidase-family hydrolase	No box	–	−4.94 ± 0.28	↓	−5.42 ± 0.50	↓	−3.23 ± 0.12	↓
	speA	RS18265	Arginine decarboxylase	AATCAATAATTCA	−766 to −739	−3.17 ± 0.36	↓	−2.47 ± 0.12	↓	−3.81 ± 0.32	↓
	speC	RS04655	Ornithine decarboxylase	No box	–	−0.70 ± 0.12	↓	−1.61 ± 0.59	↓	−2.25 ± 0.34	↓
	pmrB	RS18960	Acid pH activated two-component system sensor histidine kinase PmrB	AATCAACAGGTTA	−268 to −242	−1.94 ± 0.33	↓	−3.78 ± 0.14	↓	−2.90 ± 0.08	↓
Cell wall-degrading enzymes	*inh*	RS10815	AprI/Inh family metalloprotease inhibitor Inh	TATCAATGTCTT*T*	−84 to −58	−1.78 ± 1.31	↓	−2.27 ± 1.29	↓	−1.54 ± 0.54	↓
	pelE	RS15350	Polysaccharide lyase PelE	AATCAACTCATTG	−269 to −243	−0.04 ± 0.13	–	−0.22 ± 0.22	–	−0.46 ± 0.32	–
Type I secretion system	*prentry*	RS10810	Type I secretion system permease/ATPase Prentry	TATCAATGTCTT*T*	−463 to −437	−2.47 ± 0.20	↓	−3.27 ± 0.16	↓	−2.34 ± 0.54	↓
Type II secretion system	*gspC*	RS14420	Type II secretion system protein GspC	CATCAACCGCTTA	−723 to −697	−2.63 ± 0.08	↓	−3.52 ± 0.54	↓	−2.53 ± 0.08	↓
Type III secretion system	*hrpL*	RS11655	RNA polymerase σ factor HrpL	TAACAATTGGTTA	−234 to −208	−2.26 ± 0.04	↓	−4.34 ± 0.27	↓	−2.68 ± 0.03	↓
Type IV secretion system	*rhs*	RS03620	Type IV secretion protein Rhs	CATCAAATGTTTA	+455 to +482	−2.98 ± 0.22	↓	−4.85 ± 0.06	↓	−2.65 ± 0.11	↓
	rhs	RS06845	Type IV secretion protein Rhs	CATCAATCCGTTA	−865 to −839	−3.45 ± 0.30	↓	−4.01 ± 0.10	↓	−5.28 ± 0.15	↓
Type V secretion system	*hecB*	RS11555	HecB hemolysin secretion protein HecB	AATCAATGGGTTG	−150 to −124	−3.22 ± 0.07	↓	−4.37 ± 0.30	↓	−1.84 ± 0.36	↓
Type VI secretion syste	*hcp*	RS03605	Hcp family type VI secretion protein	AATCAAGAATTTC	−883 to −857	−5.05 ± 0.11	↓	−7.02 ± 0.23	↓	−5.01 ± 0.08	↓
Secondary metabolite synthesis	*indA*	RS00465	Indigoidine synthase IndA	TAT*T*AATCGTTTA	−268 to −241	−1.71 ± 0.13	↓	−4.62 ± 0.13	↓	−3.96 ± 0.55	↓
	hdaA	RS05020	Hypothetical protein	AAACAAAAATTTA	−224 to −197	−3.22 ± 0.14	↓	−3.11 ± 0.16	↓	−4.25 ± 0.14	↓
	hdaL	RS05075	Nonribosomal peptide synthetase	No box	–	−4.29 ± 0.44	↓	−5.37 ± 0.22	↓	−5.97 ± 0.24	↓
	fldA	RS06215	Flavodoxin FldA	AATCAACTAATTG	−35 to −9	0.56 ± 0.08	–	0.10 ± 0.09	–	0.20 ± 0.20	–

TABLE 1 (Continued)

Function category	Gene	Locus (C1O30_)	Product	Binding site (5′-WATCAANNNNTTR-3′)[a]	Position from start codon	Log$_2$ fold change of gene expression[b]					
						Δ*ihfA*		Δ*ihfB*		Δ*ihfAB*	
Motility and chemotaxis	*mcp*	RS02500	Methyl-accepting chemotaxis protein	AATCAATTAATTG	−180 to −154	−2.27 ± 0.06	↓	−3.62 ± 0.18	↓	−2.38 ± 0.24	↓
	mcp	RS02880	Methyl-accepting chemotaxis protein	TATCAATAAGTTA	−262 to −236	−3.45 ± 0.01	↓	−4.84 ± 0.39	↓	−3.21 ± 0.62	↓
	pilV	RS08665	Shufflon system plasmid conjugative transfer pilus tip adhesin PilV	TATCAATGTGTTT	−131 to −105	−3.40 ± 0.13	↓	−5.03 ± 0.16	↓	−3.18 ± 0.22	↓
	ompX	RS09065	Outer membrane protein OmpX	AATCAAAAAATTA	−243 to −217	−1.51 ± 0.07	↓	−0.87 ± 0.06	–	−0.85 ± 0.04	–
	mcp	RS09390	Methyl-accepting chemotaxis protein	TATCACCGCGTTG	−626 to −599	1.30 ± 0.34	↑	1.08 ± 1.22	↑	1.53 ± 1.06	↑
	mcp	RS12040	HAMP domain-containing protein	CATCAAATAATTG	−494 to −468	1.28 ± 0.21	↑	0.09 ± 0.06	–	0.96 ± 0.05	–
	cheA	RS13530	Chemotaxis protein CheA	TATCAAACATTTT	+5 to +31	1.49 ± 0.10	↑	1.36 ± 0.21	↑	0.01 ± 0.02	–
	flhD	RS13550	Flagellar transcriptional regulator FlhD	TATCAATTGCTTA	−485 to −459	−1.28 ± 0.14	↓	−2.51 ± 0.62	↓	−1.24 ± 0.08	↓
	mcp	RS14140	HAMP domain-containing protein	TATCAATCATTTC	−445 to −419	−0.77 ± 0.08	–	−0.97 ± 0.04	–	−0.94 ± 0.05	–
	pilT	RS17065	Type IV pilus twitching motility protein PilT	TATCCACCCCTTC	−252 to −226	−4.17 ± 0.43	↓	−5.42 ± 0.32	↓	−3.31 ± 0.12	↓
	mcp	RS20725	Methyl-accepting chemotaxis protein	AATCAAGCGCGTG	−580 to −554	−1.27 ± 0.18	↓	−2.44 ± 0.18	↓	−1.77 ± 0.16	↓
c-di-GMP	*gcpI*	RS06990	Sensor domain-containing diguanylate cyclase DGC	TATCAAGCAGTTT	−761 to −735	−1.49 ± 0.10	↓	−3.30 ± 0.18	↓	−1.72 ± 0.22	↓
	gcpJ	RS14540	Diguanylate cyclase DGC	TATCAGGTAGATA	−479 to −453	−3.46 ± 0.34	↓	−5.82 ± 0.26	↓	−4.34 ± 0.43	↓
	gcpA	RS15425	Sensor domain-containing diguanylate cyclase DGC	TATCAAAATATTA	−315 to −289	1.77 ± 0.06	↑	1.43 ± 0.18	↑	0.25 ± 0.46	–
Capsular polysaccharide synthesis	*wcaJ*	RS02585	Undecaprenyl-phosphate glucose phosphotransferase WcaJ	TATCAATCAATTT	+54 to +80	−3.34 ± 0.07	↓	−5.28 ± 0.10	↓	−4.45 ± 0.11	↓
	cpsD	RS02600	Polysaccharide biosynthesis tyrosine autokinase CpsD	CATCAACTGATTG	−97 to −71	−4.02 ± 0.58	↓	−6.00 ± 0.59	↓	−5.61 ± 0.08	↓
	/	RS02605	Capsular biosynthesis protein	TATCAACGGATTG	−300 to −274	−3.10 ± 0.14	↓	−4.81 ± 0.12	↓	−3.87 ± 0.37	↓
	/	RS02615	Glycosyltransferase	GATCAACCTTTTA	−8 to +16	−4.07 ± 0.25	↓	−5.79 ± 0.09	↓	−4.84 ± 0.26	↓
	wza	RS06590	Polysaccharide export protein Wza	CATCAACGCATTA	−131 to −105	−2.14 ± 0.36	↓	−5.02 ± 0.60	↓	−3.39 ± 0.17	↓
	wcaA	RS06605	Glycosyltransferase family 4 protein WcaA	TATCAATACCTTA	+1 to +27	−2.81 ± 0.31	↓	−2.02 ± 0.21	↓	−2.53 ± 0.33	↓
	/	RS06620	Glycosyltransferase family 2 protein	AATCAAGGCGTTT	−561 to −535	−3.30 ± 0.03	↓	−3.97 ± 0.14	↓	−2.97 ± 0.19	↓
	/	RS06690	Glycosyltransferase	AATCAAGGCGTTG	−222 to −196	−3.84 ± 0.32	↓	−2.54 ± 0.04	↓	−2.07 ± 0.06	↓

(Continues)

TABLE 1 (Continued)

Function category	Gene	Locus (C1O30_)	Product	Binding site (5′-WATCAANNNNTTR-3′)[a]	Position from start codon	Log$_2$ fold change of gene expression[b]					
						Δ*ihfA*		Δ*ihfB*		Δ*ihfAB*	
Stress resistance	*arcB*	RS01695	Aerobic respiration two-component sensor histidine kinase ArcB	AATCAGGCTGTTG	−6 to +20	−1.30 ± 0.32	↓	−1.28 ± 0.47	↓	−1.31 ± 0.34	↓
	/	RS08685	DHA2 family efflux MFS transporter permease subunit	TATCAATAGATTT	−161 to −135	−3.64 ± 0.31	↓	−4.13 ± 0.11	↓	−2.70 ± 0.07	↓
	/	RS09235	Bcr/CflA family multidrug efflux MFS transporter	AACCAACGCGTTG	−133 to −107	−3.36 ± 0.09	↓	−3.89 ± 0.36	↓	−3.72 ± 0.16	↓
	rhlA	RS09440	Biosurfactant synthesis, colonization of plant surface, alpha/beta hydrolase	TATCAAACAGTTT	−502 to −476	−3.92 ± 0.30	↓	−4.06 ± 0.14	↓	−3.64 ± 0.24	↓
	symE	RS11525	Type I toxin-antitoxin system SymE family toxin	CATCAACCGGTTG	−565 to −539	−1.94 ± 0.29	↓	−4.48 ± 0.36	↓	−2.69 ± 0.14	↓
	yafN	RS16150	Type I toxin-antitoxin system antitoxin YafN	AATCAATTTTTTG	−107 to −81	−1.97 ± 0.10	↓	−2.54 ± 0.03	↓	−1.40 ± 0.20	↓
	proV	RS16475	Glycine betaine/L-proline ABC transporter ATP-binding protein ProV	AATCAACACGTTG	−253 to −227	−1.04 ± 0.04	↓	−2.17 ± 0.04	↓	−1.61 ± 0.22	↓
	pspG	RS17225	Envelope stress response protein PspG	AATCAATGCGTTA	−138 to −112	−2.25 ± 0.37	↓	−4.69 ± 0.30	↓	−3.14 ± 0.21	↓
	robA	RS18160	MDR efflux pump AcrAB transcriptional activator RobA	AATCAAATTCTTT	−129 to −103	−1.51 ± 0.11	↓	−1.24 ± 0.03	↓	−1.84 ± 0.36	↓
Metabolic process	*xylH*	RS00425	Sugar ABC transporter permease XylH	GATCAATCAGTTG	−193 to −167	−2.74 ± 0.03	↓	−4.16 ± 0.04	↓	−2.72 ± 0.17	↓
	elbB	RS01700	Isoprenoid biosynthesis glyoxalase ElbB	AATCAATTAGTTG	−52 to −26	0.11 ± 0.02	–	−0.40 ± 0.10	–	−1.35 ± 0.05	↓
	/	RS02510	GNAT family N-acetyltransferase	TATCAACAGCTTT	−82 to −56	−3.15 ± 0.16	↓	−4.30 ± 0.08	↓	−4.72 ± 0.22	↓
	fucO	RS03185	Lactaldehyde reductase FucO	AATCAATACATTA	−41 to −15	−0.38 ± 0.24	–	−0.77 ± 0.15	–	−1.44 ± 0.17	↓
	actP	RS03385	Cation/acetate symporter ActP	TATCAACGGATTG	−307 to −281	−1.19 ± 0.06	↓	−1.68 ± 0.05	↓	−2.85 ± 0.14	↓
	phoB	RS05305	Phosphate response regulator transcription factor PhoB	TATCAGCCGGTTG	+65 to +91	−3.26 ± 0.37	↓	−3.68 ± 0.23	↓	−2.37 ± 0.05	↓
	kdpF	RS06280	K^+-transporting ATPase subunit F	CATCAATAAGTTA	−336 to −310	−2.97 ± 0.15	↓	−3.64 ± 0.21	↓	−1.90 ± 0.30	↓
	/	RS07470	SDR family oxidoreductase	AATCAAAATATTG	−165 to −139	−2.29 ± 0.37	↓	−4.48 ± 0.04	↓	−3.31 ± 0.11	↓
	hlyD	RS08935	Secretion protein HlyD	TATCAATTAGTTA	−258 to −232	0.17 ± 0.09	–	0.02 ± 0.20	–	0.35 ± 0.09	–
	deoR	RS08995	DeoR/GlpR transcriptional regulator	TATCAACTTGTTT	−182 to −156	−1.50 ± 0.03	↓	−1.58 ± 0.32	↓	−2.18 ± 0.20	↓
	dsbB	RS11160	Disulphide bond formation protein DsbB	TATCAAATAGTTA	−770 to −744	−6.45 ± 0.24	↓	−1.95 ± 0.18	↓	−1.51 ± 0.10	↓
	lctP	RS12295	L-lactate permease LctP	TATCAATAAGTTA	−50 to −24	1.97 ± 0.09	↑	0.31 ± 0.13	–	0.80 ± 0.09	–
	ptsG	RS13040	PTS sugar transporter subunit IIC PtsG	TATCAAACATTTG	−173 to −147	−1.43 ± 0.07	↓	−3.20 ± 0.12	↓	−1.80 ± 0.16	↓
	fabG	RS13300	SDR family oxidoreductase FabG	AATCAAATTTTTG	−238 to −212	−1.10 ± 0.16	↓	1.62 ± 0.07	↑	0.31 ± 0.25	–
	/	RS13660	Glycosyltransferase family 1 protein	TATCACAATCTTA	−199 to −173	−3.62 ± 0.18	↓	−4.26 ± 0.36	↓	−3.55 ± 0.03	↓
	gmhA	RS16340	D-sedoheptulose 7-phosphate isomerase GmhA	TATCAATTCATTT	−285 to −259	0.02 ± 0.14	–	−0.85 ± 0.21	–	−0.28 ± 0.26	–
	/	RS16795	D-galactonate transporter MFS	TATCAACTGGTTA	−697 to −671	−1.81 ± 0.15	↓	−1.32 ± 0.06	↓	−1.59 ± 0.35	↓
	/	RS17250	Transporter substrate-binding domain-containing protein	AATCAACGAGTTA	−125 to −99	−4.17 ± 0.37	↓	−2.13 ± 0.31	↓	−2.52 ± 0.22	↓
	aceE	RS18640	Malate synthase A AceE	AATCAAATAGTTG	−177 to −151	−0.93 ± 0.11	–	−1.62 ± 0.03	↓	−1.21 ± 0.21	↓
	/	RS20745	NAD(P)/FAD-dependent oxidoreductase	AATCAATGCATTA	−180 to −154	−1.85 ± 0.03	↓	−3.89 ± 0.10	↓	−3.01 ± 0.13	↓

TABLE 1 (Continued)

Function category	Gene	Locus (C1O30_)	Product	Binding site (5′-WATCAANNNNTTR-3′)[a]	Position from start codon	Log$_2$ fold change of gene expression[b]		
						Δ*ihfA*	Δ*ihfB*	Δ*ihfAB*
Amino acid transport	/	RS08960	ABC transporter substrate-binding protein	AATCAAAGGCTTC	−75 to −49	−2.07 ± 0.13 ↓	−2.67 ± 0.12 ↓	−1.85 ± 0.29 ↓
	/	RS09455	Aspartate:alanine antiporter	TATCAATAATTTA	−52 to −26	−1.97 ± 0.23 ↓	−2.42 ± 0.35 ↓	−1.92 ± 0.16 ↓
	/	RS13315	DegT/DnrJ/EryC1/StrS family aminotransferase	AATCAATATATTA	+68 to +94	1.09 ± 0.24 ↑	1.41 ± 0.06 ↑	1.07 ± 0.54 ↑
Replication, recombination, and repair	*cas3*	RS01885	CRISPR-associated helicase/endonuclease Cas3	AATCAACATGTTG	−366 to −340	0.56 ± 0.17 –	0.37 ± 0.18 –	−0.80 ± 0.07 –
	fxsA	RS02700	Bacteriophage exclusion-mediated protein FxsA	TATCAATGAGTTA	−51 to −25	−1.02 ± 0.14 ↓	−1.96 ± 0.16 ↓	−2.33 ± 0.12 ↓
	deoC	RS03105	Deoxyribose-phosphate aldolase DeoC	TATCAATAAGTTA	−940 to −914	−1.01 ± 0.08 ↓	−1.84 ± 0.21 ↓	−1.61 ± 0.08 ↓
	dcm	RS04625	DNA cytosine methyltransferase Dcm	AATCAACTTATTA	−360 to −334	−1.10 ± 0.08 ↓	−1.40 ± 0.06 ↓	−3.63 ± 0.02 ↓
	rof	RS04995	Rho-binding antiterminator	TATCAACCCATTA	+5 to +31	−2.38 ± 0.15 ↓	−2.18 ± 0.28 ↓	−3.22 ± 0.42 ↓
	–	RS08595	DNA-directed RNA polymerase subunit β	TATCAATTGGTTA	−137 to −111	−2.07 ± 0.09 ↓	0.53 ± 0.03 –	−2.32 ± 0.21 ↓
	/	RS08690	Integrase arm-type DNA-binding domain-containing protein	TATCAATCAGTTA	−148 to −122	−2.83 ± 0.23 ↓	−3.72 ± 0.13 ↓	−3.41 ± 0.04 ↓
	cspE	RS11295	Transcription antiterminator/RNA stability regulator CspE	AATCAAATGGTTG	−361 to −335	1.60 ± 0.19 ↑	1.49 ± 0.18 ↑	2.16 ± 0.21 ↑
	ttcA	RS12370	tRNA 2-thiocytidine(32) synthetase TtcA	AATCAATCCGTTA	−5 to +21	−3.07 ± 0.29 ↓	−1.75 ± 0.13 ↓	−2.47 ± 0.32 ↓
	/	RS16155	Site-specific integrase	AATCAAATGATTA	−118 to −82	−0.26 ± 0.09 –	−1.45 ± 0.13 ↓	−1.26 ± 0.05 ↓
	brxC	RS16230	BREX phage resistance system P-loop protein BrxC	AATCAAGAGTTTG	−262 to −236	−5.06 ± 0.47 ↓	−3.29 ± 0.40 ↓	−3.24 ± 0.47 ↓
Transcriptional regulators	*mtlR*	RS00380	MltR family transcriptional regulator	GATCAAGCCGTTG	−404 to −378	−3.56 ± 0.14 ↓	−4.95 ± 0.17 ↓	−4.80 ± 0.06 ↓
	fis	RS01395	DNA-binding transcriptional regulator Fis	ATTCAACGCCATA	−108 to −81	−4.03 ± 0.22 ↓	−4.90 ± 0.08 ↓	−4.31 ± 0.25 ↓
	slyA	RS03435	MarR family transcriptional regulator	TATCAATCAACTG	−124 to −98	−2.70 ± 0.06 ↓	−4.17 ± 0.39 ↓	−2.15 ± 0.11 ↓
	/	RS04230	LuxR C-terminal-related transcriptional regulator	AATCAAAGAATTA	−95 to −68	−3.06 ± 0.11 ↓	−5.01 ± 0.47 ↓	−3.48 ± 0.20 ↓
	/	RS04275	HxlR family transcriptional regulator	AATCAAGTTTTTC	−483 to −457	−2.60 ± 0.37 ↓	−4.48 ± 0.36 ↓	−4.01 ± 0.10 ↓
	/	RS04455	LysR family transcriptional regulator	AATCAAACCATTC	−269 to −243	−1.19 ± 0.06 ↓	−1.68 ± 0.05 ↓	−2.85 ± 0.14 ↓
	flhA	RS07705	Formate hydrogenlyase transcriptional activator FlhA	GATCAAGCTATTG	−107 to −81	−0.61 ± 0.05 –	−0.86 ± 0.04 –	−0.61 ± 0.16 –
	hnsA	RS08480	H-NS histone family protein	AATGAATATTTTA	−328 to −302	−2.45 ± 0.09 ↓	−3.58 ± 0.27 ↓	−2.00 ± 0.26 ↓
	hnsB	RS08660	H-NS histone family protein	AATGAAAAAGTGG	−154 to −128	−2.02 ± 0.09 ↓	−2.83 ± 0.08 ↓	−2.78 ± 0.22 ↓
	arsR	RS09135	Metalloregulator ArsR/SmtB family transcription factor	TATC*T*ACCTTTTA	−181 to −155	−3.83 ± 0.08 ↓	−3.88 ± 0.38 ↓	−4.48 ± 0.14 ↓
	lrp	RS09615	Leucine-responsive transcriptional regulator Lrp	AATCAATAGTTTA	−549 to −523	−2.84 ± 0.08 ↓	−0.16 ± 0.11 –	−1.41 ± 0.35 ↓
	/	RS10685	ROK family transcriptional regulator	AATCAAATATTTG	−121 to −95	0.36 ± 0.24 –	−1.25 ± 0.01 ↓	0.05 ± 0.31 –
	lysR	RS13650	LysR family transcriptional regulator	AATCAAATTATTG	−312 to −286	−3.31 ± 0.15 ↓	−4.74 ± 0.29 ↓	−3.55 ± 0.15 ↓
	pecT	RS15045	LysR family transcriptional regulator	AATCGAAATATTC	−62 to −36	−2.60 ± 0.19 ↓	−3.85 ± 0.21 ↓	−1.99 ± 0.35 ↓
	mngR	RS17210	GntR family transcriptional regulator MngR	TATCAAGGCTTT*T*	−32 to −6	−5.04 ± 0.13 ↓	−4.65 ± 0.28 ↓	−3.48 ± 0.39 ↓
	–	RS18450	MarR family transcriptional regulator	TATCAAAAGGTTA	−106 to −80	−1.35 ± 0.26 ↓	−1.26 ± 0.20 ↓	−1.92 ± 0.06 ↓

(Continues)

TABLE 1 (Continued)

Function category	Gene	Locus (C1O30_)	Product	Binding site (5′-WATCAANNNNTTR-3′)[a]	Position from start codon	Log$_2$ fold change of gene expression[b]		
						ΔihfA	*ΔihfB*	*ΔihfAB*
Hypothetical proteins	/	RS00200	DUF3861 domain-containing protein	TATCAACTATTTG	−108 to −82	−2.88 ± 0.10 ↓	−4.46 ± 0.03 ↓	−3.47 ± 0.13 ↓
	/	RS01690	TIGR01212 family radical SAM protein	AATCAATATGTTT	+4 to +30	−2.86 ± 0.13 ↓	−2.87 ± 0.16 ↓	−3.00 ± 0.23 ↓
	/	RS02900	Hypothetical protein	AATCAAAATATTA	−341 to −315	−3.61 ± 0.24 ↓	−4.14 ± 0.24 ↓	−2.99 ± 0.01 ↓
	/	RS03390	DUF485 domain-containing protein	TATCAACGGATTG	+2 to +28	−1.10 ± 0.08 ↓	−1.40 ± 0.06 ↓	−3.63 ± 0.02 ↓
	/	RS03400	Hypothetical protein	TATCAACGGTTTG	−151 to −125	−2.00 ± 0.08 ↓	−2.58 ± 0.54 ↓	−2.82 ± 0.28 ↓
	/	RS03585	Hypothetical protein	AATCAACGGGTTC	−378 to −352	−1.57 ± 0.46 ↓	−2.51 ± 0.05 ↓	−1.93 ± 0.25 ↓
	/	RS03590	Hypothetical protein	AATCAACGGGTTC	+30 to +56	−2.38 ± 0.15 ↓	−2.18 ± 0.28 ↓	−3.22 ± 0.42 ↓
	/	RS04495	IGR00645 family protein	AATCAATGTGTTA	−109 to −83	−1.62 ± 0.64 ↓	−2.82 ± 0.17 ↓	−2.67 ± 0.29 ↓
	/	RS05170	Hypothetical protein	TATCAATATCTTG	+32 to +58	−2.60 ± 0.37 ↓	−4.48 ± 0.36 ↓	−4.01 ± 0.10 ↓
	/	RS06855	Hypothetical protein	AATCAAATGATTG	−20 to +6	−1.70 ± 0.16 ↓	−3.10 ± 0.14 ↓	−1.36 ± 0.09 ↓
	/	RS06880	Hypothetical protein	GATCAATTTCTTA	−12 to +14	−6.34 ± 0.62 ↓	−4.26 ± 0.95 ↓	−4.49 ± 0.17 ↓
	/	RS07745	DUF4160 domain-containing protein	AATCAAATCATTG	−477 to −451	−2.54 ± 0.25 ↓	−3.23 ± 0.34 ↓	−3.46 ± 0.20 ↓
	/	RS08605	Hypothetical protein	AATCAACTCGTTC	−587 to −561	−0.83 ± 0.21 –	−1.52 ± 0.08 ↓	−1.91 ± 0.15 ↓
	/	RS09035	DUF1349 domain-containing protein	AATCAATACGTTA	−50 to −24	−2.38 ± 0.31 ↓	−3.82 ± 0.13 ↓	−4.29 ± 0.23 ↓
	–	RS10060	Hypothetical protein	AATCAATGAATTG	−250 to −224	−2.71 ± 0.26 ↓	−6.51 ± 1.14 ↓	−3.41 ± 0.10 ↓
	/	RS10540	YolA family protein	TATCAACTTATTG	−427 to −401	−3.00 ± 0.21 ↓	−0.63 ± 0.08 –	−1.66 ± 0.12 ↓
	/	RS10730	Hypothetical protein	AATCAACATGTTA	−58 to −32	−1.33 ± 0.26 ↓	−1.54 ± 0.13 ↓	−1.76 ± 0.17 ↓
	/	RS10850	Hypothetical protein	AATCAAATAATTA	−523 to −497	−0.95 ± 0.18 –	−1.47 ± 0.12 ↓	−3.15 ± 0.12 ↓
	/	RS11855	DUF1852 domain-containing protein	TATCAATGCATTA	−67 to −41	−1.43 ± 0.25 ↓	−0.16 ± 0.02 –	−2.61 ± 0.22 ↓
	/	RS12735	Hypothetical protein	TATCAATAGGTTG	−316 to −290	−2.58 ± 1.00 ↓	−3.95 ± 1.23 ↓	−2.14 ± 0.51 ↓
	/	RS13635	Hypothetical protein	AATCAAGAGATTA	−398 to −372	1.45 ± 0.13 ↑	0.44 ± 0.20 –	0.28 ± 0.09 –
	–	RS14145	Hypothetical protein	TATCAACGTTTTG	−291 to −265	−4.10 ± 0.06 ↓	−3.38 ± 0.18 ↓	−3.32 ± 0.21 ↓

Notes: Genes with statistically significant changes in expression (|log$_2$ fold change of expression| ≥ 1 and $p \leq 0.05$) were selected.

[a]Italics represent the mismatch of binding sites.

[b]↓ represents down-regulation of gene expression, ↑ represents up-regulation of gene expression, – represents no significant change in gene expression. Data are the results of at least three independent biological replicates and are means ± *SD*.

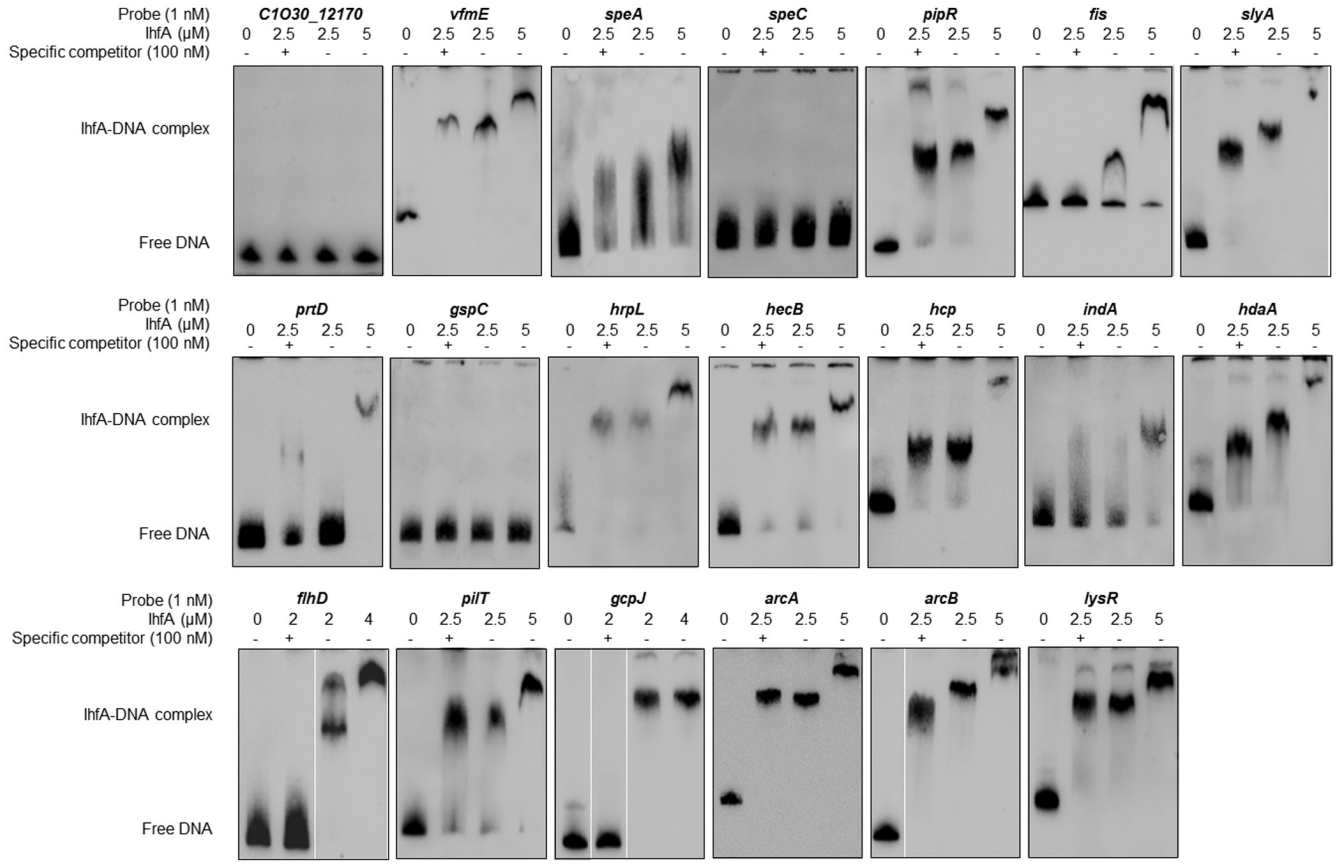

FIGURE 1 Electrophoretic mobility shift assay of IhfA protein with predicted gene promoters. 1 nM of labelled probe of *C1O30_RS12170*, *vfmE*, *speA*, *speC*, *pipR*, *fis*, *slyA*, *prtD*, *gspC*, *hrpL*, *hecB*, *hcp*, *indA*, *hdaA*, *flhD*, *pilT*, *gcpJ*, *arcA*, *arcB*, and *lysR* genes was incubated with 0–5 μM IhfA. 100 nM unlabelled corresponding probes were used as the specific competitors before adding 1 nM of the labelled probes in different reactions. The positions of free DNA and of IhfA–DNA complexes are shown

Pseudomonas (Hu et al., 2022; Waite et al., 2017). IHF is required for *hrpL* gene expression in *E. amylovora* (Lee & Zhao, 2016). In our study, a similar regulation pattern of *hrpL* was observed with 2.22–4.61 $\log_2$ fold change reduction of expression in the *ihf* mutants (Table 1). EMSA indicated that IhfA, at a concentration of 2.5 μM, directly interacted with the promoter of *hrpL* (Figure 1).

The *D. zeae* MS2 genome lacks most of the type IV secretion system (T4SS) coding genes, only retaining *virB1* (*C1O30_RS07565*), *virB2* (*C1O30_RS07560*), and two Rhs-encoding genes (*C1O30_RS03620* and *C1O30_RS06845*). The expression of these two *rhs* genes was positively regulated by IHF through the IHF motif located at 455–482 bp in the *C1O30_RS03620* open reading frame (ORF) and 865–839 bp upstream of the *C1O30_RS06845* ORF (Table 1).

Type V and type VI secretion systems (T5SS and T6SS) are both involved in contact-dependent competition (Koskiniemi et al., 2013). The former consists of two partner proteins, the HecB/TspB outer membrane protein allowing the secretion of the large HecA/TspA protein (Aoki et al., 2010). IHF positively regulated the expression of *hecB* by 1.48–4.67 $\log_2$ fold change (Table 1) and IhfA directly interacted with the promoter of *hecB* (Figure 1). In *Dickeya* spp., the T6SS comprises the secretion machinery encoded by the *imp/vas* operon, the haemolysin-coregulated protein (Hcp) and the valine-glycine repeat protein G (VgrG) that form a membrane puncturing device, and the Rhs protein effectors (Zhou et al., 2015). Deletion of *ihf* genes dramatically decreased the expression of *hcp* by 4.93–7.25 $\log_2$ fold change (Table 1). EMSA demonstrated the direct control of IhfA on *hcp* (Figure 1).

2.6 | IHF positively regulates the production of indigoidine and a novel phytotoxin

Prediction of the IHF binding motif in the MS2 genome also identified the conserved binding site in the promoter of *indA* (−268 to −242 bp upstream of the start codon). *indA* is the first gene of the *indABC* operon responsible for the biosynthesis of indigoidine, which is essential for resistance to oxidative stress (Reverchon et al., 2002). RT-qPCR analysis showed that deletion of *ihf* significantly decreased the expression of *indA* (Table 1). EMSA also verified the interaction of IhfA with the promoter of *indA* (Figure 1).

Apart from indigoidine, *D. zeae* MS2 also produces another uncharacterized secondary metabolite that inhibits the growth of *Escherichia coli* and many pathogenic fungi (Feng et al., 2019; Hu et al., 2018). The biosynthetic gene cluster has been preliminarily predicted by antiSMASH and the importance of *C1O30_RS05075* in the production of this phytotoxin has been determined (Feng

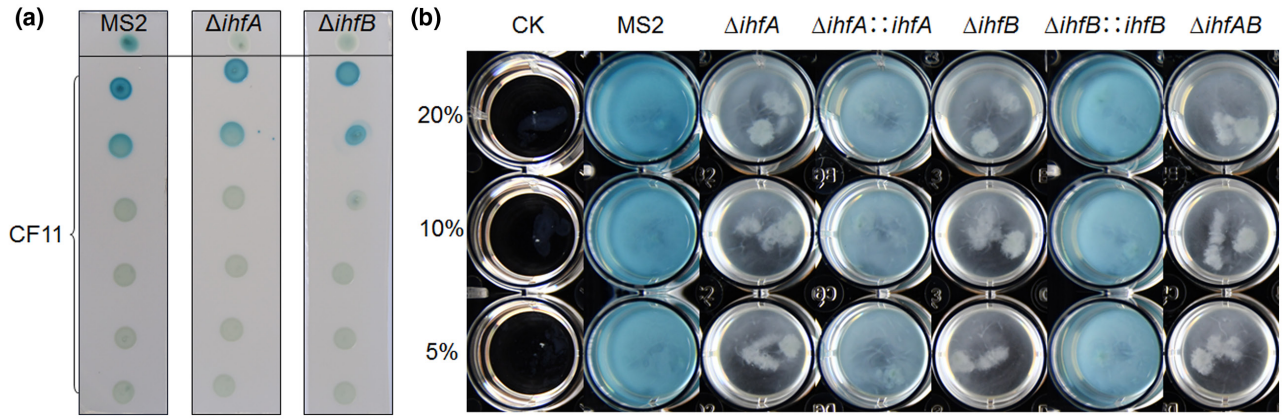

FIGURE 2 IHF regulates the production of VFM rather than the AHL quorum-sensing (QS) signal. (a) AHL signal diffusion assay of *Dickeya zeae* MS2, Δ*ihfA*, and Δ*ihfB*. Strains were spotted on the top of the agar strips and *Agrobacterium tumefaciens* CF11 (*tra-lacZ*) was used as a biosensor for the AHL QS signal (Hussain et al., 2008). (b) VFM QS signal detection of *D. zeae* MS2, Δ*ihfA*, Δ*ihfB*, Δ*ihfAB*, and complemented strains Δ*ihfA*::*ihfA* and Δ*ihfB*::*ihfB*. Different concentrations of bacterial supernatants were co-cultured with the reporter strain in medium supplemented with X-Gal at 30°C with 200 rpm for 12 h (Lv et al., 2019). CK, negative control. Experiments were repeated three times in triplicate

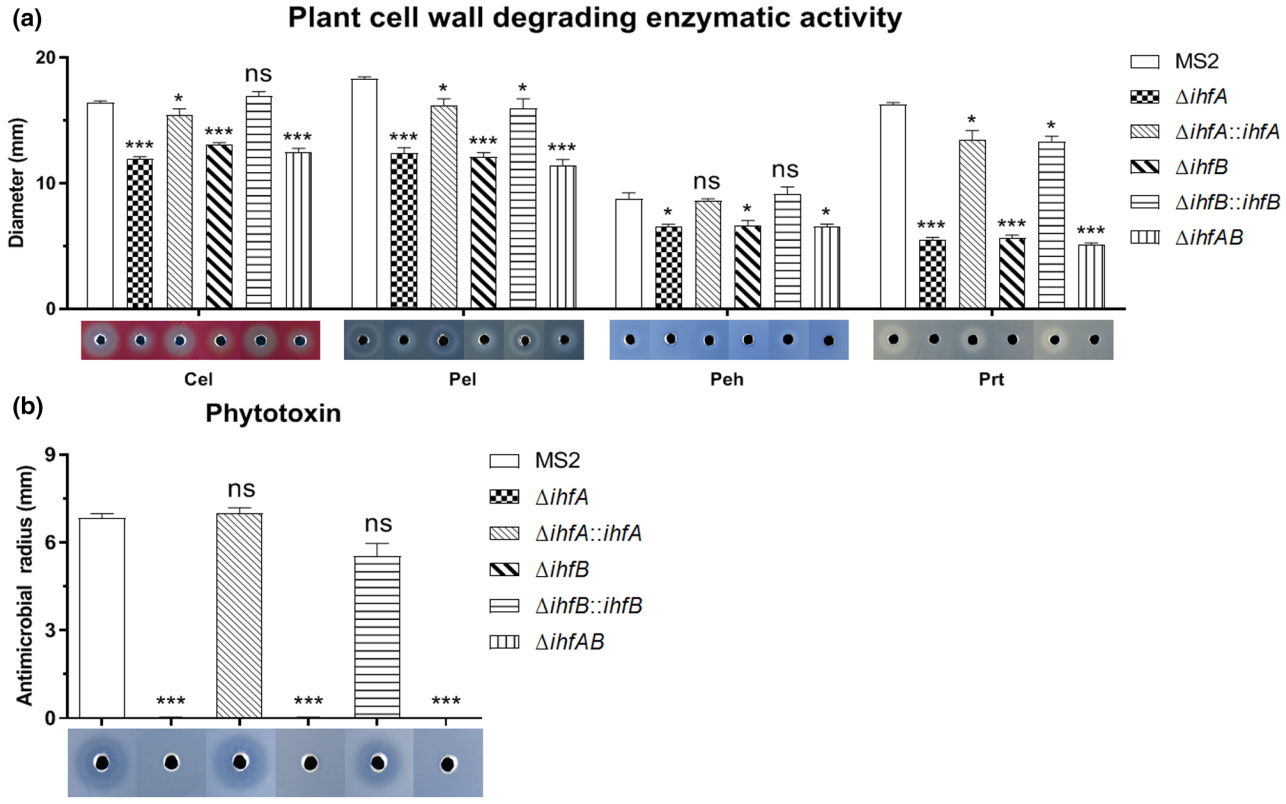

FIGURE 3 IHF regulates the production of cell wall-degrading enzymes and phytotoxin. (a) IHF contributes to cell wall degrading enzymatic activities. (b) IHF significantly modulates phytotoxin production of *Dickeya zeae* MS2. The results were averaged over the three replicates and the error bars represent standard deviations. $^{*}p < 0.05$, $^{***}p < 0.0001$; ns, not significant (Student's *t* test) ($n = 3$ independent experiments)

et al., 2019). Analysis of the organization of this gene cluster revealed that genes from *C1O30_RS05020* to *C1O30_RS05100* comprise the operon. We named these genes *hdaA*–*hdaQ*. Interestingly, an IHF binding motif was predicted in the promoter sequence of *hdaA* (*C1O30_RS05020*) (Table 1). To verify the regulation of IHF on this secondary metabolite, RT-qPCR was first performed for the expression of *hdaA* and the previously identified *hdaL* (*C1O30_RS05075*). The results showed that the expression of both *hdaA* and *hdaL* was greatly reduced, by 3.11–5.97 $\log_2$ fold change, in the *ihf* mutants compared with wild-type MS2 (Table 1). EMSA also confirmed a direct interaction of IhfA with *hdaA* (Figure 1). The production of the phytotoxin was then

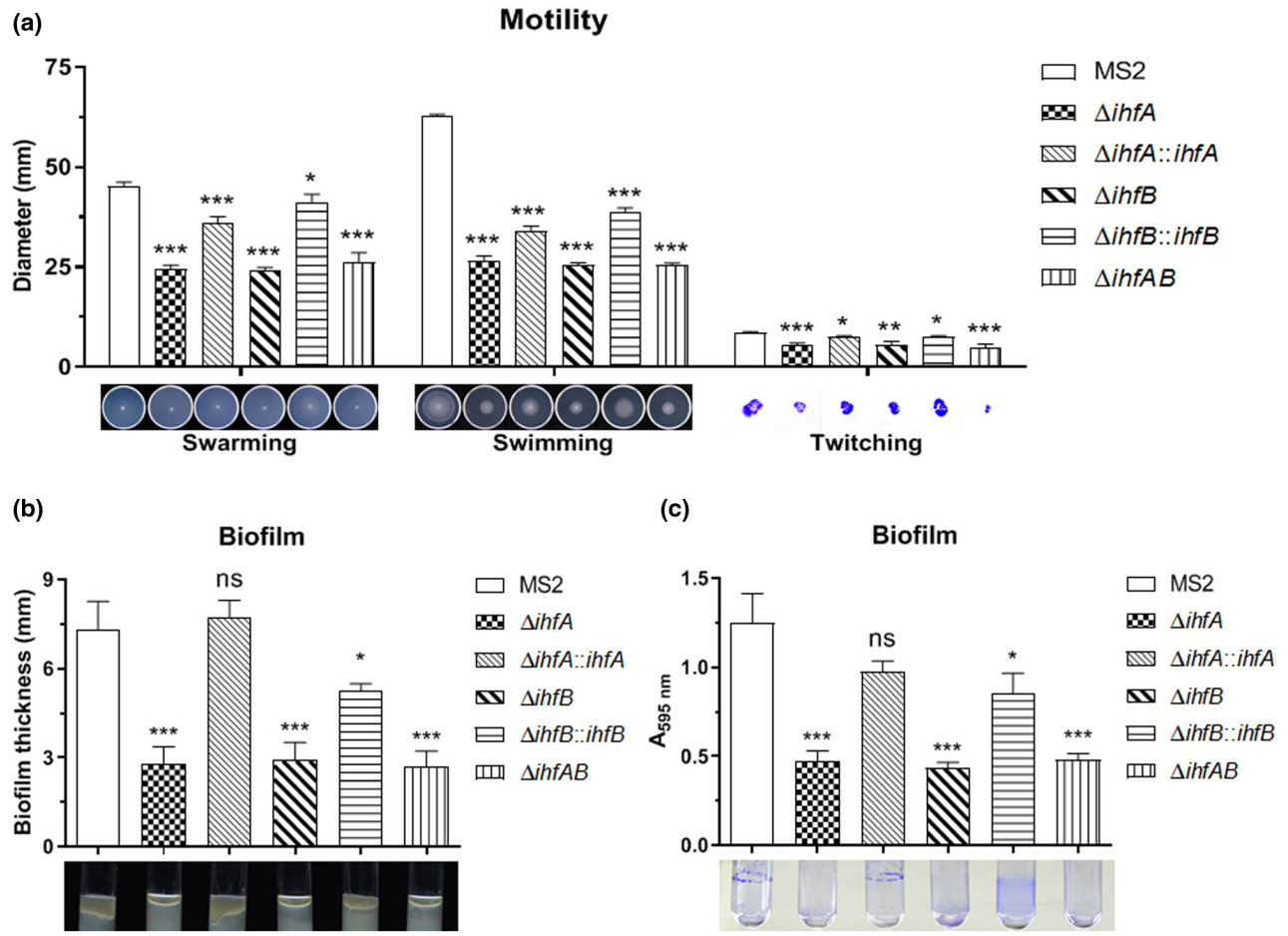

FIGURE 4 IHF regulates cell motility and biofilm formation of *Dickeya zeae* MS2. (a) Swarming, swimming, and twitching motilities of MS2 and its derivatives. (b) Nonadherent biofilms of MS2 and its derivatives formed at the air/liquid interface. (c) Attached biofilms of MS2 and its derivatives measured by crystal violet staining. The experimental results were averaged over the three replicates and the error bars represent standard deviations (*SD*). $^{*}p<0.05$, $^{**}p<0.001$, $^{***}p<0.0001$; ns, not significant (Student's *t* test) ($n = 3$ independent experiments)

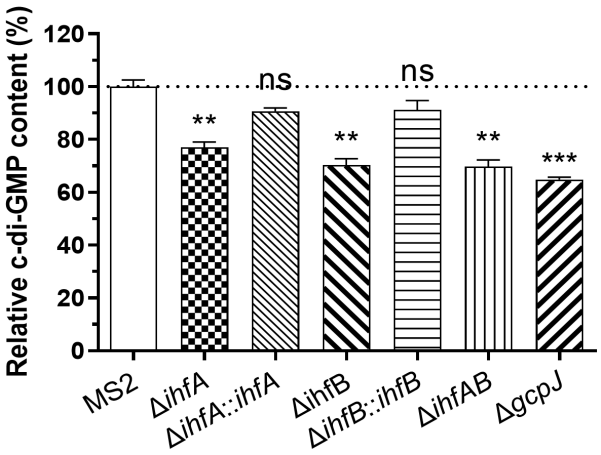

FIGURE 5 Deletion of *ihf* genes and *gcpJ* decreases c-di-GMP concentration in *Dickeya zeae* MS2. c-di-GMP concentrations of mutants and complemented stains were normalized to that of the wild-type MS2, which was set to 100%. The experimental results were averaged over the three replicates and the error bars represent standard deviations (*SD*). $^{**}p<0.001$, $^{***}p<0.0001$, ns, not significant (Student's *t* test) ($n = 3$ independent experiments)

measured and significantly reduced production was observed as expected (Figure 3b).

2.7 | Mutation of *ihf* reduces cell motility and biofilm formation

Surface motility, biofilm formation, and host invasion are some of the manifestations of functional responses to surface colonization (Harshey, 2003). Biofilm formation is important for bacteria to survive in a harsh environment and attach to the host surface, while bacterial motility is one of the major determinants for pathogen diffusion and invasion. In this study, we tested whether cell motility and biofilm formation were affected by IHF. As shown in Figure 4a, all the *inf* mutants (Δ*ihfA*, Δ*ihfB*, and Δ*ihfAB*) exhibited an obvious decrease in swimming, swarming, and twitching motility; complementation of *ihfA* and *ihfB* into the corresponding mutants partially recovered cell motility. In addition, the nonadherent and attached biofilms formed by the deletion mutants were much less than wild-type MS2 and the complemented strains (Figures 4b and 5c).

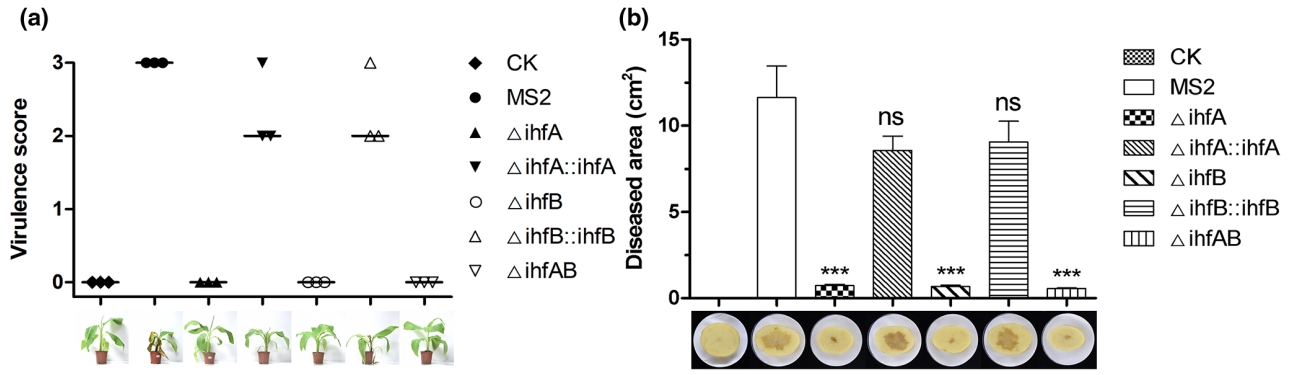

FIGURE 6 Deletion of *ihf* genes reduces the virulence of *Dickeya zeae* MS2. (a) Virulence of MS2 and *ihf* mutants on banana seedlings. Each banana seedling was inoculated with 200 μl of fresh bacterial culture (OD_{600} 1.0) and kept in an incubator at 28°C with 12-h alternating light–dark cycles for 14 days. Three biological replicates were set for each treatment. The virulence scoring method was described by Feng et al. (2019). (b) Virulence of MS2 and *ihf* mutants on potato slices. Each potato slice was inoculated with 2 μl of bacterial culture (OD_{600} 1.0) and kept at 28°C under moist conditions. The area of lesions was measured using ImageJ v. 1.52a after 24 h. CK, negative control. ***$p < 0.0001$; ns, not significant (Student's *t* test) ($n = 3$ independent experiments)

Motility and chemotaxis are essential for bacteria when searching for favourable niches to invade plants. During this process, flagella-mediated movement is vital and under the control of multiple regulatory systems. FlhDC is the master regulator of flagellar genes controlling cell motility, CWDE expression, and the T3SS in *D. dadantii* 3937 (Yuan et al., 2015). In this study, the expression of *flhD* was 1.24–2.51 $\log_2$ fold change decreased in the *ihf* muants (Table 1). Moreover, 4 μM of IhfA bound to the promoter of *flhD* (Figure 1), suggesting direct control of IHF on flagella-mediated motility. Furthermore, *pilT*, which encodes type IV pili that contribute to twitching motility, was decreased in expression by over 3.31 $\log_2$ fold change in the *ihf* mutants (Table 1); EMSA also verified a direct interaction of IhfA with *pilT* at a concentration of 2.5 μM (Figure 1).

Cyclic-di-GMP (c-di-GMP) is a second messenger chemical in bacteria, playing an important role in cell division, motility, and virulence regulation. The turnover of c-di-GMP in bacterial cells is effected by its synthesis by diguanylate cyclases (DGCs) and degradation by phosphodiesterases (PDEs). DGC catalyses the formation of c-di-GMP through a conserved GGDEF domain (Tal et al., 1998). Previous investigations have characterized the repertoires of c-di-GMP turnover genes in the *D. dadantii* 3937 and *D. oryzae* EC1 genomes (Chen et al., 2016; Yi et al., 2010). Like the EC1 strain, the genome of *D. zeae* MS2 harbours 12 GGDEF domain proteins, three EAL domain proteins, and three GGDEF-EAL hybrid proteins (Chen et al., 2016). Among the genes encoding these proteins, only three, *C1O30_RS06990* (*gcpI*, with dCache_1 and GGDEF domains), *C1O30_RS14540* (*gcpJ*, with TM, GGDEF, and d2mhr_ domains), and *C1O30_RS15425* (*gcpA*, with PAS, PAC, GAF and GGDEF domains), have the IHF binding motif in their promoter regions (Table 1). RT-qPCR analysis showed that the expression of *gcpI* and *gcpJ* was significantly reduced in the *ihf* mutants (Table 1). In *D. oryzae* EC1, IHF protein has been reported to bind to the promoter region of a DGC protein (Chen et al., 2019) that is a homologue of GcpJ. EMSA confirmed the direct binding of IhfA to the promoter of *gcpJ* (Figure 1). To determine whether IHF affects the c-di-GMP level of MS2, we measured the c-di-GMP concentrations of the wild-type strain and its derivatives. The results showed that deletion of *ihfA*, *ihfB* or both decreased the production of c-di-GMP by about 23%–31%, and deletion of *gcpJ* resulted in a decrease by about 35%. Complementation of *ihfA* and *ihfB* in corresponding mutants recovered the c-di-GMP production (Figures 5 and S2).

The methyl-accepting chemotaxis protein (MCP) is one of the key proteins of microbial cell-sensing chemical signals in the external environment and is able to change the rotation direction of the bacterial flagellum. In strain MS2, six *mcp* genes possess the IHF binding motif in their promoter regions and three (*C1O30_RS02500*, *C1O30_RS02880*, and *C1O30_RS20725*) had significantly decreased expression in the *ihf* mutants, while the expression of *C1O30_RS09390* was increased (Table 1).

Interestingly, a gene encoding an aerobic respiration two-component sensor histidine kinase, *arcB*, was also predicted to contain the IHF binding motif in the promoter. The expression of *arcB* was obviously reduced in the *ihf* mutants (Table 1), implicating the positive regulation of IHF on ArcB. In *Serratia marcescens* FS14, ArcB promotes bacterial motility by activating the synthesis of flagella and the expression of the biosurfactant serrawettin W1, while its cognate response regulator ArcA could not (Zhang et al., 2018). These results are the reverse of those found in *E. coli*, in which ArcA is necessary for the expression of flagellum-specific sigma factor FliA while ArcB appears not to be involved in motility (Kato et al., 2007). ArcAB also controls the anaerobic growth of *E. coli* and the resistance to reactive oxygen species (ROS) of *Salmonella* (Loui et al., 2009). In *D. zeae* MS2, both *arcA* and *arcB* directly interacted with IhfA (Figure 1).

2.8 | IHF mediates capsular polysaccharide synthesisCPS and stress resistance of *D. zeae* MS2

Capsular polysaccharide is an essential virulence factor for pathogenesis of bacteria and plays a role in protecting bacteria against

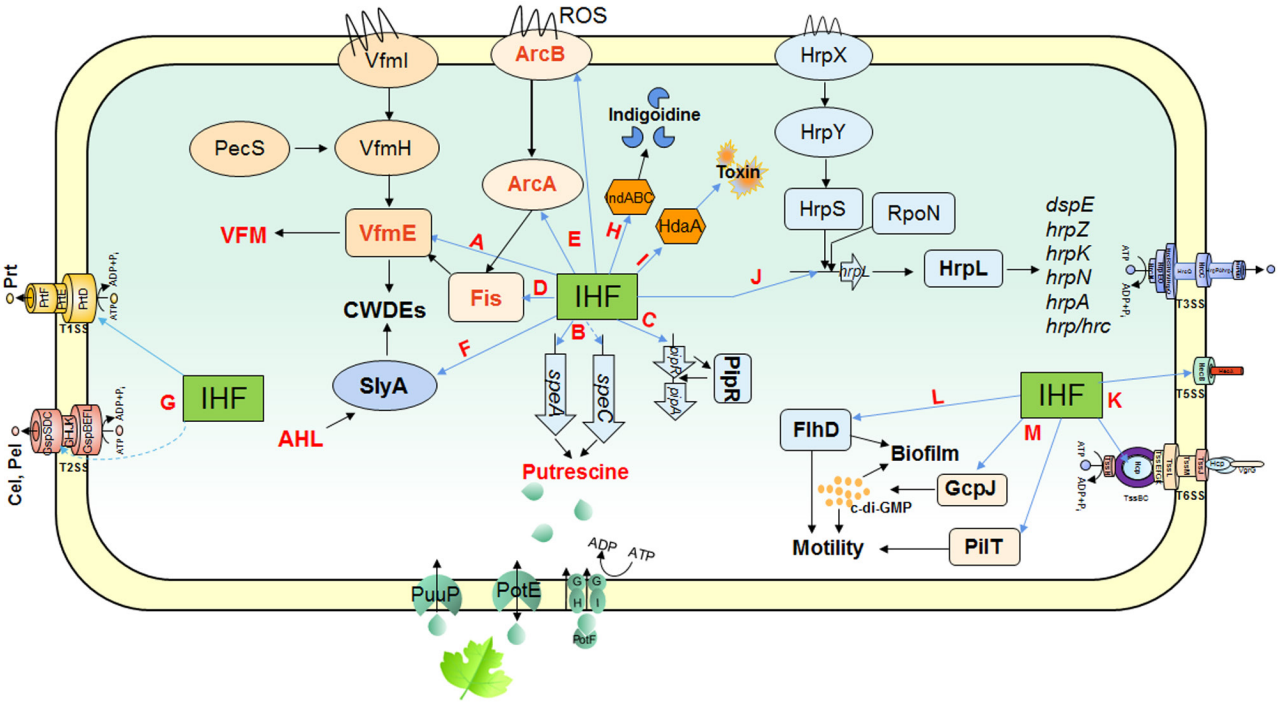

FIGURE 7 The regulatory network of IHF in *Dickeya zeae* MS2. IHF directly binds to the promoter of *vfmE* and affects the biosynthesis of VFM quorum-sensing (QS) signal (A), directly interacts with the promoter of *speA* and indirectly interacts with *speC* to modulate the intracellular putrescine signal level (B), directly binds to the promoter region of the *luxR*-solo homologue *pipR* (C), regulates the production of cell wall-degrading enzymes (CWDEs) via multiple regulatory pathways including IHF-VfmE, IHF-Fis/IHF-Fis-VfmE (D), IHF-ArcAB-Fis (E), IHF-SlyA (F), IHF-PrtD (T1SS)/IHF-GspC (type II secretion system) (G), directly binds to the *indA* promoter to regulate production of indigoidine (H), regulates the production of phytotoxin by direct binding to the *hdaA* promoter (I), directly binds the *hrpL* promoter and acts as an enhancer to activate *hrpL* expression, thus affecting type III secretion system effector secretion to the extracellular environment (J), and directly binds to *hecB* and *hcp* (k). IHF regulates cell motility and biofilm formation by directly binding to the *flhD* promoter (L), the c-di-GMP encoding gene *gcpJ*, and the *pilT* (M)

phagocytosis and environmental stresses. The biosynthesis of capsular polysaccharides involves multiple genes. In strain MS2, eight genes related to the biosynthesis of capsular polysaccharides were identified as containing the IHF binding motif and all of them were positively regulated by IHF (Table 1). Toxin-antitoxin operons are ubiquitous in bacteria and their products can cause cell growth arrest (Zhang et al., 2012). Expression of *yafN* and *symE*, which encode two toxin-antitoxin proteins, was activated by IHF (Table 1). Furthermore, a multidrug resistance (MDR) efflux pump AcrAB transcriptional activator, RobA, was also identified as positively regulated by IHF because its expression was reduced in the *ihf* mutants (Table 1). RobA has been reported to positively regulate the most important MDR efflux pump in *E. coli* (Tanaka et al., 1997). Altogether, the above results suggest the possibility of a deficiency of stress resistance in *ihf* mutants.

2.9 | IHF mediates the metabolic process of *D. zeae* MS2

A significant decrease in *ihf* mutants of the expression of genes involved in the metabolic pathway that achieves redox potential (NADPH) and energy transfer (*xylH*, *ptsG*, *fucO*, *phoB*, *deoR*, *dsbB* and *fldA*, encoding various carbohydrate transporter enzymes and oxidoreductases and their intermediates) was observed (Table 1). It is worth mentioning that *aceE*, encoding a malate synthase, *C1O30_RS02510*, encoding an acetyltransferase (GNAT) family member, and *kdpF*, encoding a transport ATPase, were also activated by IHF (Table 1), suggesting that IHF may influence the tricarboxylic acid cycle and thus affect the growth of *D. zeae* MS2 (Figure S1).

2.10 | Deletion of IHF affects bacterial pathogenicity

The above characteristics, such as the Vfm QS system (Lv et al., 2019), the LuxR-solo system (Feng et al., 2019), CWDE (Hu et al., 2022), and the unknown phytotoxin (Hu et al., 2018), motility and biofilm formation, and the c-di-GMP level (Chen et al., 2016), are known to play important roles in *Dickeya* virulence. Thus, we hypothesized that IHF would mediate the virulence of *D. zeae* MS2. To determine whether deletion of *ihfA* and *ihfB* affected the invasive ability of MS2, we inoculated banana seedlings and potato slices with the same amount of MS2, Δ*ihfA*, Δ*ihfB*, Δ*ihfAB* and the complemented strains. According to the virulence scoring method described previously (Feng et al., 2019), the disease severity of the banana seedlings inoculated with the mutants was ranked "0"

(symptomless) after 7 days of inoculation, while the banana seedlings inoculated with MS2 and the complemented strains were discoloured and rotten (Figure 6a). At 24 h postinoculation, the diseased area on the potato slices inoculated with the three deletion mutants was much smaller than those slices inoculated with MS2 or the complemented strains (Figure 6b), indicating that the deletion of *ihf* genes reduced the ability of MS2 to infect potato slices. We also measured the weights of the diseased tissue on potato slices caused by wild-type strain MS2 and its derivatives and calculated the colony-forming units (cfu) of the bacteria in the diseased tissues. The average weights of the diseased potato tissues inoculated by MS2, Δ*ihfA*, Δ*ihfB*, Δ*ihfAB*, Δ*ihfA*::*ihfA*, and Δ*ihfB*::*ihfB* were 1.428, 0.049, 0.218, 0.014, 1.029, and 1.575 g, respectively. The cfu in each gram of diseased tissues was slightly less following inoculation with Δ*ihfA* and Δ*ihfAB* than those inoculated with the other strains (Figure S3). The result of the pathogenicity tests showed that deletion of *ihf* in *D. zeae* caused it to almost lose its pathogenicity to dicotyledonous and monocotyledonous hosts.

3 | DISCUSSION

In early studies, IHF was thought to be an integration protein in *E. coli* playing an important role in the integration of phage DNA into the host chromosome (Craig & Nash, 1984; Gamas et al., 1986; Yang & Nash, 1989). It can specifically recognize a consensus motif (5′-WATCAANNNNTTR-3′) in the genome (Craig & Nash, 1984; Yang & Nash, 1989) and induce DNA bends. The conserved proline residues on the two subunits of IHF protein can be inserted between DNA base pairs, resulting in a sharp 140° distortion of DNA (Ali et al., 2001; Dixit et al., 2005; Ellenberger & Landy, 1997). By 2000, further functions of IHF had been discovered in bacteria. In *Brucella abortus*, IHF is involved in the transcriptional regulation of the *virB* operon of the T4SS (Sieira et al., 2004). In *Pseudomonas syringae* pv. *phaseolicola*, IHF binds to the promoter of the *phtD* operon to mediate the synthesis of phaseolotoxin (Arvizu-Gómez et al., 2011). In *Geobacter sulfurreducens*, duplicated IhfA and IhfB proteins affect bacterial respiration, physiological function, and extracellular electron transfer (Andrade et al., 2021).

Although the gene coding sequences of IHF were described in *D. dadantii* 3937 in 1994 (Douillie et al., 1994), little research on the function of IHF was reported in *Dickeya* until recently. In *D. oryzae* EC1, deletion of IHF resulted in decreased production of biofilms, CWDEs, and zeamines, and IHF was found to bind to the gene encoding a DGC, affecting the signal transduction of second messenger c-di-GMP (Chen et al., 2019). In *D. dadantii* 3937, IHF is capable of affecting the expression of genes required for virulence and pectin catabolism, and thus regulates the pathogenicity (Reverchon et al., 2021). The findings in this study showed a similar result in that IHF in *D. zeae* MS2 was required for virulence (Figure 6), production of CWDEs (Figure 3a), bacterial motility, and biofilm formation (Figure 4). Additional new functions of IHF were found, positively regulating the production of VFM and putrescine QS signals (Figures 1 and 2), indigoidine (Figure 1) and an MS2-specific phytotoxin (Figures 1 and 3b), and the secretion systems from T1SS to T6SS (Figure 1 and Table 1). IHF modulates diverse phenotypes in *D. zeae* MS2, for instance the biosynthesis of VFM QS signal (Figure 2b) by direct binding to the promoter of *vfmE* (Figures 1 and 7a), the putrescine signal level by direct interaction with the *speA* promoter and indirect interaction with *speC* (Table 1, Figures 1 and 7b), the *luxR*-solo system by direct interaction with the *pipR* promoter (Figure 7c), the production of CWDEs through multiple regulatory pathways, including IHF-VfmE, IHF-Fis/IHF-Fis-VfmE (Figure 7d), IHF-ArcAB-Fis (Figure 7e), IHF-SlyA (Figure 7f), and IHF-PrtD (T1SS)/IHF-GspC (T2SS) (Figure 7g), the production of indigoidine by direct binding to the *indA* promoter (Figure 7h), and the production of a phytotoxin by direct binding to the *hdaA* promoter (Figure 7i). Moreover, IHF directly bound the *hrpL* promoter and acted as an enhancer to activate *hrpL* expression, thus affecting T3SE secretion to the extracellular environment (Figure 7j), and regulated the expression of *rhs*, *hecB*, and *hcp* (Table 1 and Figure 7k). Cell motility and biofilm formation were also regulated by direct interaction of IhfA with the promoters of *flhD* (Figures 1 and 7l), the c-di-GMP encoding gene *gcpJ*, and the *pilT* (Figures 1, 5, and 7m). The findings in this study revealed many important target genes directly bound by IhfA protein, which encode pathogenicity regulatory factors manipulating and coordinating the virulence programming of *D. zeae* MS2, suggesting an important role of IHF as a master regulator in *Dickeya*. Interestingly, IhfA directly acted on the production of both VFM and putrescine QS signals to mediate CWDE production and flagella-triggered infection, respectively, which strongly contribute to the virulence of *Dickeya* (Lv et al., 2019; Shi et al., 2019).

In *E. coli* K12, IHF, along with Lrp, H-NS, Fis, FNR, CRP, and ArcA, are located in the top level of the transcriptional regulatory network from the regulonDB database (http://regulondb.ccg.unam.mx/menu/tools/transcritional_regulation_network/images/NetWorkTFGene.jpeg) (Martınez-Antonio & Collado-Vides, 2003; Salgado et al., 2006). In this study, IHF has been found to interact with H-NS, Fis, and ArcA (Table 1, Figures 1 and 7). Such synergistic or antagonistic roles of IHF with other master regulators, even NAPs, have also been observed in other bacterial pathogens. In *Salmonella enterica*, IHF alleviates the inhibition of H-NS on *hilA* expression, which is important for pathogen virulence (Queiroz et al., 2011). Additionally, in *E. coli*, IHF assists EcpR to promote its binding to the *ecp* promoter and activate fimbriae gene transcription. The interaction between IHF and EcpR can offset the inhibitory effect of H-NS on *ecp* expression (Martínez-Santos et al., 2012). In *S. marcescens* FS14 and *E. coli*, ArcAB TCS regulates most of the genes in the tricarboxylic acid cycle and affects bacterial motility and virulence factor production (Loui et al., 2009; Zhang et al., 2018). This may also be another reason for the slow growth of *ihf* mutants in addition to the IHF-regulated genes involved in the metabolic process.

In *Pseudomonas*, PipR is a member of the LuxR-solo transcription factor family capable of responding to plant-produced compounds to mediate the expression of peptidase genes (Schaefer et al., 2016). Although there is no evidence proving the direct reception of PipR to specific host elements, we believe that IHF is involved in the

TABLE 2 Strains and plasmids used in this study

Strain or plasmid	Relevant description[a]	Source or reference
Strains		
Dickeya zeae		
MS2	Wild type of *Dickeya zeae*	Laboratory stock
Δ*ihfA*	A deletion mutant derived from MS2	This study
Δ*ihfB*	A deletion mutant derived from MS2	This study
Δ*ihfAB*	A deletion mutant derived from MS2	This study
Δ*ihfA*::*ihfA*	Δ*ihfA* containing plasmid construct pLAFR-*ihfA*, Tc^r	This study
Δ*ihfB*::*ihfB*	Δ*ihfB* containing plasmid construct pLAFR-*ihfB*, Tc^r	This study
Escherichia coli		
CC118λ	*Δ(ara-leu) araDΔ(lacX74 galE galK phoA20 thi-1 rpsE rpoB argE (Am) recA λpir*	Laboratory stock
DH5α	*supE44ΔlacU169* (ϕ80*lacZ*ΔM15), *hsdR17 recA1 endA1 gyrA96 thi-1 relA1 λpir*	Laboratory stock
BL21(DE3)	A protein expression host for efficient exogenous genes with T7 RNA polymerase as the expression system, Kan^r	Laboratory stock
Plasmids		
pKNG101	R6K *ori*, *sacB* (Suc^s), Str^r	Laboratory stock
pET28b	N-His, N-thrombin, N-T7, C-His, Kan^r	Laboratory stock
pRK2013	Auxiliary vector, Kan^r	Laboratory stock
pLAFR3	Expression vector containing a pt*ac*TAC promoter, Tc^r	Laboratory stock

[a]Tc^r, Kan^r, Str^r indicate resistance to tetracycline, kanamycin, or streptomycin, respectively. Suc^s indicates sensitivity to sucrose.

plant–*Dickeya* transkingdom interactions through the LuxR-solo system. More associations need further in-depth research.

From the EMSA results, IhfA protein bound to DNA in the form of a monomer at low concentration and in the form of a polymer at high concentration in most cases (Figure 1). Some of the DNA regions that interacted with IhfA contain multiple putative IHF binding sites, such as the promoters of *fis*, *hdaA*, *flhD*, *pilT*, *gcpJ*, and *arcB*. However, there is no direct evidence that polymer formation of the IHF–DNA complex is specifically related to the number of binding sites. This nature of the IHF–DNA complexes is similar to those characterized in *D. dadantii* 3937 and *Desulfovibrio vulgaris* (Fiévet et al., 2014; Reverchon et al., 2021). IHF, as a NAP, binds DNA with loose specificity to modulate the transcriptional activity of bacterial genes by modification of the chromosome architecture (Reverchon et al., 2021). A recent study demonstrated that only the fully wrapped (147° of DNA bend) binding mode occurs with sequence specificity (Yoshua et al., 2021). It is expected that future research will reveal the mechanism of action of IHF and the discovery of more NAPs in microorganisms.

In summary, the findings from this study reveal the contribution of IHF to the pathogenic process, and dissect the regulation networks, in *D. zeae* MS2. IHF controls the production of VFM and putrescine QS signals by direct binding to the *vfmE* and *speA* promoters, affects phytotoxin and indigoidine production by direct binding to the *hdaA* and *indA* promoters, and interacts with the LuxR-solo system, Fis, SlyA, and FlhD transcriptional regulators directly, and with the T1SS–T6SS directly or indirectly. These findings highlight the importance of IHF in virulence regulation and add new insight to the sophisticated regulation pathways that control *Dickeya* virulence.

4 | EXPERIMENTAL PROCEDURES

4.1 | Bacterial growth conditions and antibiotic concentrations

The strains used in this study are listed in Table 2. *D. zeae* MS2 and its derivatives were cultured at 28°C in Luria-Bertani (LB) medium and minimal medium (MM) (Zhou et al., 2016). *E. coli* strains were cultured at 37°C in LB medium. Antibiotics were added to the medium at the following final concentrations when required: tetracycline (Tc) 15 μg/ml, streptomycin (Sm) 50 μg/ml, polymyxin B sulphate (Pm) 25 μg/ml, and kanamycin (Km) 100 μg/ml.

4.2 | Bacterial plasmids, mutant and complemented strain construction

Plasmids used in this study are listed in Table 2 and the primers used in this study are listed in Table S2. To knock out the ORF of *ihfA* and *ihfB*, 5′ and 3′ flanking fragments of *ihfA* and *ihfB* genes were amplified from MS2 genomic DNA. The two purified fragments and the *Bam*HI/*Spe*I digested suicide plasmid pKNG101 were ligated using a ClonExpress MultiS kit (Vazyme Biotech Co.). The ligation product was then transferred into the *E. coli* CC118λ competent cells by 42°C heat shock and subsequently cultured in LB medium supplemented with 50 μg/ml Sm for approximately 4 h before spreading on LB agar supplemented with 50 μg/ml Sm. A positive transformant was co-cultured with wild-type MS2 and the helper plasmid pRK2013 by triparental mating (Lv et al., 2018). Mutants were selected on MM agar medium supplemented with 5% sucrose and confirmed by PCR and DNA sequencing. Similarly, triparental conjugation was used to delete *ihfB* based on the existing mutant Δ*ihfA* to obtain the double-knockout mutant Δ*ihfAB*. To construct the complemented strains, the coding regions of the genes *ihfA* and *ihfB* were amplified with the primers listed in Table S2 and then ligated to the *Bam*HI/*Eco*RI-digested plasmid pLAFR3. The ligated DNA mixtures were separately transformed into *E. coli* DH5α competent cells, and positive transformants were then selected on LB agar supplemented with 15 μg/ml Tc. The recombinant plasmids were introduced into corresponding mutants by triparental mating. The complemented strains were selected on MM agar supplemented with 15 μg/ml Tc and confirmed by PCR. The deletion mutants and complemented strains were confirmed by DNA sequencing at Sangon Biotech.

4.3 | Prediction of the IHF binding sites in the MS2 genome

fimo v. 5.1.0 was used to search for the IHF binding motif in the MS2 genome (GCF_002887555.1_ASM288755v1) (Grant et al., 2011). The motifs were filtered to identify those located at −600 to +100 bp from a CDS and harbouring ≥10 bp of A/T in the −26 to −14 bp upstream of the motifs.

4.4 | RNA purification and RT-qPCR

MS2 and the mutants were cultured at 28°C in LB medium to an OD_{600} of 1.0. Total bacterial RNA was extracted using Eastep Super Total Extraction Kit (Promega), and the concentration of RNA was measured using a Nano-500 microspectrophotometer (Aosheng), samples were visualized by agarose gel electrophoresis to confirm complete bands, and then stored at −80°C. Any contaminating genomic DNA was removed from the RNA samples using FastKing gDNA Dispelling RT SuperMix FastKing (Tiangen) and then cDNA was synthesized, and the resultant cDNA fragments were stored at −20°C. The qPCR was prepared using ChamQ SYBR qPCR Master Mix (Vazyme) according to the product instructions. The reaction procedure was performed in a QuantStudio 12 K Flex real-time PCR instrument (Life Technologies). The qPCR primers used in the experiment are listed in Table S2 and the experimental data were processed using the $2^{-\Delta\Delta Ct}$ method (Livak & Schmittgen, 2001).

4.5 | EMSA

EMSA was performed using the methods in previous studies (Hu et al., 2022; Lv et al., 2019; Nasser & Reverchon, 2002). In detail, the coding region of *ihfA* was amplified with the primers listed in Table S2 using MS2 genomic DNA as the template. The amplified fragment was ligated to the *Bam*HI/*Eco*RI-digested vector pET28b, transformed into *E. coli* BL21 (DE3) competent cells, and then grown on LB agar plates supplemented with 50 μg/ml Km overnight. The colonies were confirmed by PCR using the primers pET28b-F/R (Table S2). *E. coli* BL21 (DE3) containing the *ihfA*-coding fragment was grown at 37°C with 200 rpmshaking in 1 L of LB medium containing 50 μg/ml Km to OD_{600} of 0.6, then 1 mM IPTG was added into the medium and the cells were transferred to 18°C with shaking at 170 rpm to induce *ihfA* expression. All culture grown overnight was transferred into tubes for centrifugation at 1630 × *g* for 40 min and resuspended in appropriate volume of phosphate-buffered saline (PBS) twice. The cells were resuspended in 30 ml of PBS and disrupted by an ultrasonic cell breaker for 20 min with pulse for 6 s and pause for 2 s. The crude protein product after fragmentation by sonication was checked for the presence of the target protein on a 10% PAGE gel. Protein purification was performed at 4°C. The crude protein extract was mixed with Ni NTA beads. PBS containing low to high concentrations of imidazole (10, 50, 100, 150, 200, 300, and 500 mM) were added sequentially to the Ni NTA beads. The effluent at each concentration of imidazole was collected and analysed on a 10% PAGE gel. The protein samples were aliquoted into 1.5-ml tubes and stored at −80°C.

The promoter regions ranging from 200 to 300 bp of the target genes containing the IHF binding sites were amplified using the primers listed in Table S2. Purified promoter fragments were labelled using the biotin 3′-end labeling kit (Thermo Fisher). A reaction system with a total volume of 10 μl was then prepared using the LightShift Chemiluminescence EMSA kit (Thermo Fisher). PCR fluid contained 1 μl of LightShift 10× Binding Buffer, 0.5 μl of LightShift Poly (dI-dC), 1 nM labelled probe, 0–5 μM IhfA, and distilled water. The reaction mixture was incubated at 22°C for 30 min while the competition reaction mixture containing 100 nM unlabelled probe was incubated with the protein for 10 min before adding 1 nM labelled probe to complete the remaining reaction. The reaction product was run for 1–1.5 h in a 6% nondenaturing polyacrylamide gel at 90 V and then transferred onto a PVDF membrane at 80 V for 2.5 h. After cross-linking to the positively charged PVDF membrane by UV-light cross-linker (CX-200 UV Crosslinker), a Chemiluminescent Nucleic Acid Detection Module (Thermo Fisher) was used. The experimental results were observed with a chemiluminescence instrument (Tanon).

4.6 | AHL and VFM bioassays

The AHL signal was detected using the method previously described (Hussain et al., 2008), where 20 ml of MM agar supplemented with 20 µl of X-Gal (40 mg/ml) was poured into a 9-cm diameter Petri dish under light-avoidance conditions. After solidification, the medium was cut into 1-cm wide separate slices. *Agrobacterium tumefaciens* CF11 containing a *tra-lacZ* fusion gene was used as a biosensor for the AHL signal. Equal amounts of freshly cultured CF11 at OD_{600} 0.1 were spotted on the separate slices. MS2, Δ*ihfA*, and Δ*ihfB* at OD_{600} 1.0 were spotted on the front of the CF11. The dish was incubated at 28°C for 24 h. The blue spots of the biosensor indicated the production of the AHL signal. To determine whether deletion of *ihf* genes affected VFM signal generation, the reporter strain with *lacZ* substituted for *vfmE* in Δ*lacZ* of *D. oryzae* EC1 was used in this study (Lv et al., 2019). First, 1 ml of MM was added to each well of a 24-well tissue culture plate (BIOFIL). Next, 1 µl of X-Gal and 10 µl of 6-h cultured reporter strain were added to the medium. Then MS2 and *ihf* mutant supernatants in final concentrations of 5%, 10%, and 20% were added to the medium. The plate was shaken at 30°C and 200 rpm for 12 h. The assays were repeated three times in triplicate.

4.7 | Measurement of PCWDE activity

The CWDE activity of the *ihf* mutants was measured as described previously (Chatterjee et al., 1995; Lv et al., 2018), but where the protease (Prt) assay medium was adjusted as a mixture of 3% agar LB medium and 4% skimmed milk. Thirty microlitres of cellulase (Cel), pectate lyase (Pel), polygalacturonase (Peh), and protease (Prt) assay media were poured into each 13 × 13 cm square Petri dish. After drying in a vertical flow clean bench, 5-mm diameter holes were made on the solid media with a sterilized hole puncher. The agar in the holes was picked out with a sterilized toothpick. Fresh wild-type MS2, mutants, and complemented strains were grown to OD_{600} of 1.0 and the cultures were then centrifuged for 10 min at 1300 × *g* and 4°C. The obtained supernatants were filtered through a 0.22-µm membrane filter. Forty microlitres of the supernatants were added to the holes. The dishes were put in a 28°C incubator for 14–16 h. To observe the results, the Pel and Peh assay plates were soaked in 1 M HCl for 15 min, while the Cel assay plates were soaked in 0.1% (wt/vol) Congo red solution for 15 min. Subsequently, the three kinds of assay plates were washed twice with 1 M NaCl before observation. The Prt activity results were observed without any treatment. The radii of the halos were measured and collated with ImageJ v. 1.52a software. The assay was repeated three times in triplicate.

4.8 | Phytotoxin assay

Previous studies revealed that *D. zeae* MS2 produces a novel phytotoxin as one of the virulence factors towards rice seeds and banana (Feng et al., 2019; Hu et al., 2018). To test whether IHF regulates this phytotoxin production, we first prepared a phytotoxin detection medium containing a mixture of 1.5% agar LB medium and 1% agarose. Next, 500 µl of fresh *E. coli* DH5α was mixed into 50 ml of phytotoxin detection medium (50–60°C) and poured into a 13 × 13 cm square Petri dish. Then 5-mm diameter holes were made on the solid medium with a sterilized hole puncher and 20 µl of supernatants of bacteria (OD_{600} of 1.0 in MM) were applied to the holes. Dishes were incubated overnight at 37°C. The radii of the clear bacterial inhibition zone on the medium were measured using ImageJ v. 1.52a. The assay was repeated three times in triplicate.

4.9 | Measurement of cell motility and biofilm formation

Bacterial swimming and swarming motility were tested on semisolid medium according to the method described previously (Hussain et al., 2008). The medium recipe was slightly adjusted to accommodate the strain characteristics in this study. Specifically, 15 ml of swimming medium (Bacto peptone 5 g/L, NaCl 5 g/L, Bacto agar 2.5 g/L) was poured into a 9-cm diameter Petri dish. Strains were grown to OD_{600} 1.0 and 1 µl of bacterial cultures was stabbed into the centre of the semisolid medium after it was nearly air-dried. The same volume of bacterial cultures was added to the surface of the swarming medium (tryptone 10 g/L, NaCl 5 g/L, agarose 4 g/L) plates. The plates were put in a 28°C incubator for 10–12 h. The diameters of bacterial swimming and swarming were measured with ImageJ v. 1.52a. Twitching motility was tested based on the method described previously (Rashid & Kornberg, 2000). A bacterial colony from overnight 1.5% (wt/vol) LB agar plates was inoculated with a sterilized toothpick to the bottom of a fresh 1.5% (wt/vol) LB agar plate and cultured at 28°C for 24 h. The twitching area was measured by ImageJ v. 1.52a to calculate the diameter of the area.

To quantify the biofilms formed by MS2 and its mutants, strains were grown in LB medium to OD_{600} 1.0, 40 µl of which was added to 14-ml glass tubes containing 4 ml of SOBG medium (tryptone 20 g/L, yeast extract 5 g/L, $MgSO_4$ 1.2 g/L, NaCl 0.5 g/L, KCl 0.186 g/L, glycerol 20 ml/L). The glass tubes were rested on a table for 48 h. Because biofilms produced by the wild-type MS2 and its derivatives do not stick well to the tube walls, we measured the nonadherent biofilms formed at the air/liquid interface. Under static conditions, biofilms of MS2 and its derivatives were formed on the surface of the SOBG medium. The thickness of the biofilms floating on the medium surface was measured using ImageJ v. 1.52a. The assay was repeated three times in triplicate. To quantitatively measure the attached biofilms, we modified the method described previously (O'Toole & Kolter, 1998). Briefly, cultures were removed and the glass tubes were washed by flowing water, then 200 ml of 0.1% crystal violet (wt/vol) was added into the glass tubes and incubated at room temperature for 15 min. The dye was removed and the glass tubes were washed by flowing water. The glass tubes were thoroughly dried at 60°C, then 1 ml of 95% ethanol was added to

completely dissolve the biofilm and subsequently aliquoted into a 96-well plate with 200 µl solute per well. The quantity of biofilm formation was determined by measuring the absorbance at 595 nm. The assay was repeated three times in triplicate.

4.10 | Quantitative analysis of c-di-GMP by LC–MS

c-di-GMP was measured following a previous study with slight modifications (Chen et al., 2022). Overnight bacterial culture was diluted in 1:100 in 10 ml of MM and strains were grown to OD_{600} 0.6–0.8 at 28°C, 200 rpm. Cell lysis was performed by adding perchloric acid (70% vol/vol) to a final concentration of 0.6 M for 30 min at 4°C. Samples were centrifuged at 3900 × *g* for 10 min and the supernatants were collected. After the pH was neutralized by adding 1/5 volume of 2.5 M $KHCO_3$, the samples were centrifuged at 1300 × *g* at 4°C for 10 min. The supernatant was loaded in a 1.5-ml centrifuge tube, centrifuged again at 3900 × *g* at 4°C for 10 min, and the supernatants were collected for liquid chromatography-mass spectrometry (LC–MS/MS) analysis.

LC–MS/MS was undertaken using a Q Exactive Focus hybrid quadrupole-orbitrap mass spectrometer (Thermo Fisher Scientific) with a 1.8 µm, 100×2.1 mm high-strength silica (HSS) T3 column (ACQUITY UPLC; Waters). A gradient system was used for isocratic elution with 95% aqueous (2.5 mM ammonium acetate) and 5% organic (methanol), with a 0.2 ml/min flow rate and a 7 min cycle time. c-di-GMP was detected by Orbitrap mass analyser on a Q Exactive Focus system under positive ionization mode. Ten microlitres of the sample were injected and the *m/z* 691 > 248 transition was used for quantification.

For generation of a standard curve, 0, 2.5, 5, 10, 25, 50, 100, 250, 500, and 1000 nM of pure c-di-GMP (Biolog) with 0.1% formic acid were analysed as described above. c-di-GMP levels were normalized to total protein per millilitre of culture. Data were expressed as the means of three independent cultures with error bars indicating the standard deviation.

For protein quantification, precipitated fractions were resuspended in 1 M NaOH and heated in a water bath at about 100°C. The protein lysate was quantified using a Bradford protein assay kit (Dingguo Biology) according to the manufacturer's instructions. The experiment was performed in triplicate. GraphPad Prism v. 5 was used to perform significance difference analysis and mapping.

4.11 | Pathogenicity determination

Based on the properties of MS2 (Hu et al., 2018), potato slices and banana seedlings were selected as representative host plants in this study. Banana seedlings were purchased from Fruit Research Institute, Guangdong Academy of Agricultural Sciences, Guangzhou, China. The pathogenicity test on banana seedlings and virulence scoring of the disease used the methods described previously with minor modifications (Feng et al., 2019). Before performing the experimental processing, banana seedlings were first transplanted to plastic pots in an incubator at 28°C with 12-h alternating light–dark cycles. Fresh wild-type MS2, mutants, and complemented strains were cultured to OD_{600} 1.0, then 200 µl of which was added to 1-ml sterile syringes, and injected into the base of the banana pseudostems. LB medium was used as the negative control. Treated banana seedlings were grown in an incubator at 28°C with 12-h alternating light–dark cycles for 14 days. Pictures were taken daily to record the disease incidence of the plants. Three biological replicates were set for each treatment.

The pathogenicity test on potato was performed as follows. First, healthy potatoes were washed, cut into slices about 5 mm thick, put into 9-cm diameter Petri dishes covered with clean filter paper, and then placed into a vertical-flow clean bench to air-dry the surface water. Next, the needle of a 1-ml sterile syringe was cut to approximately 1 mm in length and then stabbed into the centre of the potato slices to create a surface wound. Fresh wild-type MS2, mutants, and complemented strains were grown to OD_{600} 1.0 and 2 µl of the culture was applied to the potato wound. LB medium was used as the negative control. Potato slices were incubated at 28°C for 24 h. The diseased area was measured using ImageJ v. 1.52a (Schneider et al., 2012). Each treatment was performed in triplicate.

To quantify the cfu of MS2 and its mutants in the potato slices, the diseased tissues were cut using a sterile knife, weighed and ground, and then diluted with sterile water, 100 µl of which was spread onto LB agar plates and cultured at 28°C for 24 h. Plates with colony numbers between 30 and 300 were selected to count the cfu. Each treatment was performed in triplicate.

ACKNOWLEDGEMENTS

This work was financially supported by grants from the National Natural Science Foundation of China (31972230), the Key-Area Research and Development Program of Guangdong Province (2020B0202090001 and 2018B020205003), the Natural Science Foundation of Guangdong Province, China (2020A1515011534), the Guangzhou Basic Research Program (202102080613), and the China Scholarship Council Fellowship Program Grant (202108440367).

CONFLICT OF INTEREST

The authors declare that there are no known conflicts of interest associated with this paper.

DATA AVAILABILITY STATEMENT

The data that support the findings of this study are available from the corresponding author upon reasonable request.

ORCID

Jianuan Zhou https://orcid.org/0000-0001-9774-330X

REFERENCES

Ali, B.M.J., Amit, R., Braslavsky, I., Oppenheim, A.B., Gileadi, O. & Stavans, J. (2001) Compaction of single DNA molecules induced

by binding of integration host factor (IHF). *Proceedings of the National Academy of Sciences of the United States of America*, 98, 10658–10663.

Andrade, A., Hernández-Eligio, A., Tirado, A.L., Vega-Alvarado, L., Olvera, M., Morett, E. et al. (2021) Specialization of the reiterated copies of the heterodimeric integration host factor genes in *Geobacter sulfurreducens*. *Frontiers in Microbiology*, 12, 626443.

Aoki, S.K., Diner, E.J., de Roodenbeke, C.T.K., Burgess, B.R., Poole, S.J., Braaten, B.A. et al. (2010) A widespread family of polymorphic contact-dependent toxin delivery systems in bacteria. *Nature*, 468, 439–442.

Arvizu-Gómez, J.L., Hernández-Morales, A., Pastor-Palacios, G., Brieba, L.G. & Álvarez-Morales, A. (2011) Integration Host Factor (IHF) binds to the promoter region of the *phtD* operon involved in phaseolotoxin synthesis in *P. syringae* pv. *phaseolicola* NPS3121. *BMC Microbiology*, 11, 90.

Chatterjee, A., Cui, Y., Liu, Y., Dumenyo, C.K. & Chatterjee, A.K. (1995) Inactivation of *rsmA* leads to overproduction of extracellular pectinases, cellulases, and proteases in *Erwinia carotovora* subsp. *carotovora* in the absence of the starvation/cell density-sensing signal, N-(3-oxohexanoyl)-L-homoserine lactone. *Applied and Environmental Microbiology*, 61, 1959–1967.

Chen, Y., Lv, M., Liao, L., Gu, Y., Liang, Z., Shi, Z. et al. (2016) Genetic modulation of c-di-GMP turnover affects multiple virulence traits and bacterial virulence in rice pathogen *Dickeya zeae*. *PLoS One*, 11, e0165979.

Chen, X., Yu, C., Li, S., Li, X. & Liu, Q. (2019) Integration host factor is essential for biofilm formation, extracellular enzyme, zeamine production, and virulence in *Dickeya zeae*. *Molecular Plant-Microbe Interactions*, 32, 325–335.

Chen, Y., Lv, M., Liang, Z., Liu, Z., Zhou, J. & Zhang, L. (2022) Cyclic di-GMP modulates sessile-motile phenotypes and virulence in *Dickeya oryzae* via two PilZ domain receptors. *Molecular Plant Pathology*, 23, 870–884.

Craig, N.L. & Nash, H.A. (1984) *E. coli* integration host factor binds to specific sites in DNA. *Cell*, 39, 707–716.

Dey, D., Nagaraja, V. & Ramakumar, S. (2017) Structural and evolutionary analyses reveal determinants of DNA binding specificities of nucleoid-associated proteins HU and IHF. *Molecular Phylogenetics and Evolution*, 107, 356–366.

Dixit, S., Singh-Zocchi, M., Hanne, J. & Zocchi, G. (2005) Mechanics of binding of a single integration-host-factor protein to DNA. *Physical Review Letters*, 94, 118101.

Douillie, A., Toussaint, A. & Faelen, M. (1994) Identification of the integration host factor genes of *Erwinia chrysanthemi* 3937. *Biochimie*, 76, 1055–1062.

Ellenberger, T. & Landy, A. (1997) A good turn for DNA: the structure of integration host factor bound to DNA. *Structure*, 5, 153–157.

Feng, L., Schaefer, A.L., Hu, M., Chen, R., Greenberg, E.P. & Zhou, J. (2019) Virulence factor identification in the banana pathogen *Dickeya zeae* MS2. *Applied and Environmental Microbiology*, 85, e01611–19.

Fiévet, A., Cascales, E., Valette, O., Dolla, A. & Aubert, C. (2014) IHF is required for the transcriptional regulation of the *Desulfovibrio vulgaris* Hildenborough *orp* operons. *PLoS One*, 9, e86507.

Friedman, D.I. (1988) Integration host factor: a protein for all reasons. *Cell*, 55, 545–554.

Gamas, P., Burger, A.C., Churchward, G., Caro, L., Galas, D. & Chandler, M. (1986) Replication of pSC101: effects of mutations in the *E. coli* DNA binding protein IHF. *Molecular and General Genetics*, 204, 85–89.

German Sanchez, D., David Primo, E., Teresa Damiani, M. & Teresita Lisa, A. (2017) *Pseudomonas aeruginosa gbdR* gene is transcribed from a σ^{54}-dependent promoter under the control of NtrC/CbrB, IHF and BetI. *Microbiology*, 163, 1343–1354.

Grant, C.E., Bailey, T.L. & Noble, W.S. (2011) FIMO: scanning for occurrences of a given motif. *Bioinformatics*, 27, 1017–1018.

Harshey, R.M. (2003) Bacterial motility on a surface: many ways to a common goal. *Annual Review of Microbiology*, 57, 249–273.

Hommais, F., Oger-Desfeux, C., Van Gijsegem, F., Castang, S., Ligori, S., Expert, D. et al. (2008) PecS is a global regulator of the symptomatic phase in the phytopathogenic bacterium *Erwinia chrysanthemi* 3937. *Journal of Bacteriology*, 190, 7508–7522.

Hu, M., Li, J., Chen, R., Li, W., Feng, L., Shi, L. et al. (2018) *Dickeya zeae* strains isolated from rice, banana and clivia rot plants show great virulence differentials. *BMC Microbiology*, 18, 136.

Hu, M., Xue, Y., Li, C., Lv, M., Zhang, L., Parsek, M.R. et al. (2022) Genomic and functional dissections of *Dickeya zeae* shed light on the role of type III secretion system and cell wall-degrading enzymes to host range and virulence. *Microbiology Spectrum*, 10, e159021.

Hugouvieux-Cotte-Pattat, N., Condemine, G., Nasser, W. & Reverchon, S. (1996) Regulation of pectinolysis in *Erwinia chrysanthemi*. *Annual Review of Microbiology*, 50, 213–257.

Hussain, M.B.B.M., Zhang, H., Xu, J., Liu, Q., Jiang, Z. & Zhang, L. (2008) The acyl-homoserine lactone-type quorum-sensing system modulates cell motility and virulence of *Erwinia chrysanthemi* pv. *zeae*. *Journal of Bacteriology*, 190, 1045–1053.

Kato, Y., Sugiura, M., Mizuno, T. & Aiba, H. (2007) Effect of the *arcA* mutation on the expression of flagella genes in *Escherichia coli*. *Bioscience Biotechnology and Biochemistry*, 71, 77–83.

Koskiniemi, S., Lamoureux, J.G., Nikolakakis, K.C., de Roodenbeke, C.T., Kaplan, M.D., Low, D.A. et al. (2013) Rhs proteins from diverse bacteria mediate intercellular competition. *Proceedings of the National Academy of Sciences of the United States of America*, 110, 7032–7037.

Lee, J.H. & Zhao, Y. (2016) Integration host factor is required for RpoN-dependent *hrpL* gene expression and controls motility by positively regulating *rsmB* sRNA in *Erwinia amylovora*. *Phytopathology*, 106, 29–36.

Lin, B.R., Shen, H.F., Pu, X.M., Tian, X.S., Zhao, W.J., Zhu, S.F. et al. (2010) First report of a soft rot of banana in mainland China caused by a *Dickeya* sp. (*Pectobacterium chrysanthemi*). *Plant Disease*, 94, 640.

Liu, F., Hu, M., Zhang, Z., Xue, Y., Chen, S., Hu, A. et al. (2022) *Dickeya* manipulates multiple quorum sensing systems to control virulence and collective behaviors. *Frontiers in Plant Science*, 13, 838125.

Livak, K.J. & Schmittgen, T.D. (2001) Analysis of relative gene expression data using real-time quantitative PCR and the $2^{-\Delta\Delta CT}$ method. *Methods*, 25, 402–408.

Login, F.H., Fries, M., Wang, X., Pickersgill, R.W. & Shevchik, V.E. (2010) A 20-residue peptide of the inner membrane protein OutC mediates interaction with two distinct sites of the outer membrane secretin OutD and is essential for the functional type II secretion system in *Erwinia chrysanthemi*. *Molecular Microbiology*, 76, 944–955.

Lory, S. (1998) Secretion of proteins and assembly of bacterial surface organelles: shared pathways of extracellular protein targeting. *Current Opinion in Microbiology*, 1, 27–35.

Loui, C., Chang, A.C. & Lu, S. (2009) Role of the ArcAB two-component system in the resistance of *Escherichia coli* to reactive oxygen stress. *BMC Microbiology*, 9, 183.

Lv, M., Chen, Y., Liao, L., Liang, Z., Shi, Z., Tang, Y. et al. (2018) Fis is a global regulator critical for modulation of virulence factor production and pathogenicity of *Dickeya zeae*. *Scientific Reports*, 8, 341.

Lv, M., Hu, M., Li, P., Jiang, Z., Zhang, L.H. & Zhou, J. (2019) A two-component regulatory system VfmIH modulates multiple virulence traits in *Dickeya zeae*. *Molecular Microbiology*, 111, 1493–1509.

Martinez-Antonio, A. & Collado-Vides, J. (2003) Identifying global regulators in transcriptional regulatory networks in bacteria. *Current Opinion in Microbiology*, 6, 482–489.

Martínez-Santos, V.I., Medrano-López, A., Saldaña, Z., Girón, J.A. & Puente, J.L. (2012) Transcriptional regulation of the *ecp* operon by EcpR, IHF, and H-NS in attaching and effacing *Escherichia coli*. *Journal of Bacteriology*, 194, 5020–5033.

Mikkel, K., Tagel, M., Ukkivi, K., Ilves, H. & Kivisaar, M. (2020) Integration Host Factor IHF facilitates homologous recombination and mutagenic processes in *Pseudomonas putida*. *DNA Repair*, 85, 102745.

Nasser, W. & Reverchon, S. (2002) H-NS-dependent activation of pectate lyases synthesis in the phytopathogenic bacterium *Erwinia chrysanthemi* is mediated by the PecT repressor. *Molecular Microbiology*, 43, 733–748.

Nasser, W., Dorel, C., Wawrzyniak, J., Van Gijsegem, F., Groleau, M., Deziel, E. et al. (2013) Vfm a new quorum sensing system controls the virulence of *Dickeya dadantii*. *Environmental Microbiology*, 15, 865–880.

Oliveira Monteiro, L.M., Sanches-Medeiros, A., Westmann, C.A. & Silva-Rocha, R. (2020) Unraveling the complex interplay of Fis and IHF through synthetic promoter engineering. *Frontiers in Bioengineering and Biotechnology*, 8, 510.

O'Toole, G.A. & Kolter, R. (1998) Initiation of biofilm formation in *Pseudomonas fluorescens* WCS365 proceeds via multiple, convergent signalling pathways: a genetic analysis. *Molecular Microbiology*, 28, 449–461.

Palacios, J.L., Zaror, I., Martinez, P., Uribe, F., Opazo, P., Socias, T. et al. (2001) Subset of hybrid eukaryotic proteins is exported by the type I secretion system of *Erwinia chrysanthemi*. *Journal of Bacteriology*, 183, 1346–1358.

Prieto, A.I., Kahramanoglou, C., Ali, R.M.R., Fraser, G.M., Seshasayee, A.S.N. & Luscombe, N.M. (2012) Genomic analysis of DNA binding and gene regulation by homologous nucleoid-associated proteins IHF and HU in *Escherichia coli* K12. *Nucleic Acids Research*, 40, 3527–3537.

Queiroz, M.H., Madrid, C., Paytubi, S., Balsalobre, C. & Juárez, A. (2011) Integration host factor alleviates H-NS silencing of the *Salmonella enterica* serovar Typhimurium master regulator of SPI1, *hilA*. *Microbiology*, 157, 2504–2514.

Rashid, M.H. & Kornberg, A. (2000) Inorganic polyphosphate is needed for swimming, swarming, and twitching motilities of *Pseudomonas aeruginosa*. *Proceedings of the National Academy of Sciences of the United States of America*, 97, 4885–4890.

Reverchon, S., Bouillant, M.L., Salmond, G. & Nasser, W. (1998) Integration of the quorum-sensing system in the regulatory networks controlling virulence factor synthesis in *Erwinia chrysanthemi*. *Molecular Microbiology*, 29, 1407–1418.

Reverchon, S., Rouanet, C., Expert, D. & Nasser, W. (2002) Characterization of indigoidine biosynthetic genes in *Erwinia chrysanthemi* and role of this blue pigment in pathogenicity. *Journal of Bacteriology*, 184, 654–665.

Reverchon, S., Meyer, S., Forquet, R., Hommais, F., Muskhelishvili, G. & Nasser, W. (2021) The nucleoid-associated protein IHF acts as a 'transcriptional domainin' protein coordinating the bacterial virulence traits with global transcription. *Nucleic Acids Research*, 49, 776–790.

Rice, P.A., Yang, S., Mizuuchi, K. & Nash, H.A. (1996) Crystal structure of an IHF-DNA complex: a protein-induced DNA U-turn. *Cell*, 87, 1295–1306.

Richet, E., Abcarian, P. & Nash, H.A. (1986) The interaction of recombination proteins with supercoiled DNA: defining the role of supercoiling in integrative recombination. *Cell*, 46, 1011–1021.

van Rijn, P.A., Goosen, N. & van de Putte, P. (1988) Integration host factor of *Escherichia coli* regulates early- and repressor transcription of bacteriophage Mu by two different mechanisms. *Nucleic Acids Research*, 16, 4595–4605.

van Rijsewijk, B.R.B.H., Nanchen, A., Nallet, S., Kleijn, R.J. & Sauer, U. (2011) Large-scale C-13-flux analysis reveals distinct transcriptional control of respiratory and fermentative metabolism in *Escherichia coli*. *Molecular Systems Biology*, 7, 477.

Rodionov, D.A., Gelfand, M.S. & Hugouvieux-Cotte-Pattat, N. (2004) Comparative genomics of the KdgR regulon in *Erwinia chrysanthemi* 3937 and other gamma-proteobacteria. *Microbiology*, 150, 3571–3590.

Salgado, H., Santos-Zavaleta, A., Gama-Castro, S., Peralta-Gil, M., Peñaloza-Spínola, M.I., Martínez-Antonio, A. et al. (2006) The comprehensive updated regulatory network of *Escherichia coli* K-12. *BMC Bioinformatics*, 7, 5.

Samson, R., Legendre, J.B., Christen, R., Fischer-Le Saux, M., Achouak, W. & Gardan, L. (2005) Transfer of *Pectobacterium chrysanthemi* (Burkholder et al. 1953) Brenner et al. 1973 and *Brenneria paradisiaca* to the genus *Dickeya* gen. nov as *Dickeya chrysanthemi* comb. nov and *Dickeya paradisiaca* comb. nov and delineation of four novel species, *Dickeya dadantii* sp. nov., *Dickeya dianthicola* sp. nov., *Dickeya dieffenbachiae* sp. nov. and *Dickeya zeae* sp. nov. *International Journal of Systematic and Evolutionary Microbiology*, 55, 1415–1427.

Schaefer, A.L., Oda, Y., Coutinho, B.G., Pelletier, D.A., Weiburg, J., Venturi, V. et al. (2016) A LuxR homolog in a cottonwood tree endophyte that activates gene expression in response to a plant signal or specific peptides. *mBio*, 7, e01101–16.

Schneider, C.A., Rasband, W.S. & Eliceiri, K.W. (2012) NIH Image to ImageJ: 25 years of image analysis. *Nature Methods*, 9, 671–675.

Shi, Z., Wang, Q., Li, Y., Liang, Z., Xu, L., Zhou, J. et al. (2019) Putrescine is an intraspecies and interkingdom cell-cell communication signal modulating the virulence of *Dickeya zeae*. *Frontiers in Microbiology*, 10, 1950.

Sieira, R., Comerci, D.J., Pietrasanta, L.I. & Ugalde, R.A. (2004) Integration host factor is involved in transcriptional regulation of the *Brucella abortus virB* operon. *Molecular Microbiology*, 54, 808–822.

Tal, R., Wong, H.C., Calhoon, R., Gelfand, D., Fear, A.L., Volman, G. et al. (1998) Three *cdg* operons control cellular turnover of cyclic Di-GMP in *Acetobacter xylinum*: genetic organization and occurrence of conserved domains in isoenzymes. *Journal of Bacteriology*, 180, 4416–4425.

Tanaka, T., Horii, T., Shibayama, K., Sato, K., Ohsuka, S., Arakawa, Y. et al. (1997) RobA-induced multiple antibiotic resistance largely depends on the activation of the AcrAB efflux. *Microbiology and Immunology*, 41, 697–702.

Waite, C., Schumacher, J., Jovanovic, M., Bennett, M. & Buck, M. (2017) Negative autogenous control of the master type III secretion system regulator HrpL in *Pseudomonas syringae*. *mBio*, 8, e02273-16.

Wang, X., Pineau, C., Gu, S., Guschinskaya, N., Pickersgill, R.W. & Shevchik, V.E. (2012) Cysteine scanning mutagenesis and disulfide mapping analysis of arrangement of GspC and GspD protomers within the type 2 secretion system. *The Journal of Biological Chemistry*, 287, 19082–19093.

Yang, C.C. & Nash, H.A. (1989) The interaction of *E. coli* IHF protein with its specific binding sites. *Cell*, 57, 869–880.

Yi, X., Yamazaki, A., Biddle, E., Zeng, Q. & Yang, C.H. (2010) Genetic analysis of two phosphodiesterases reveals cyclic diguanylate regulation of virulence factors in *Dickeya dadantii*. *Molecular Microbiology*, 77, 787–800.

Yoshua, S.B., Watson, G.D., Howard, J.A.L., Velasco-Berrelleza, V., Leake, M.C. & Noy, A. (2021) Integration host factor bends and bridges DNA in a multiplicity of binding modes with varying specificity. *Nucleic Acids Research*, 49, 8684–8698.

Yuan, X., Khokhani, D., Wu, X., Yang, F., Biener, G., Koestler, B.J. et al. (2015) Cross-talk between a regulatory small RNA, cyclic-di-GMP signalling and flagellar regulator FlhDC for virulence and bacterial behaviours. *Environmental Microbiology*, 17, 4745–4763.

Zhang, F., Xing, L., Teng, M. & Li, X. (2012) Crystallization and preliminary crystallographic studies of the YafN-YafO complex from *Escherichia coli*. *Acta Crystallographica Section F: Structural Biology and Crystallization Communications*, 68, 894–897.

Zhang, J., Lin, B., Shen, H. & Pu, X. (2013) Genome sequence of the banana pathogen *Dickeya zeae* strain MS1, which causes bacterial soft rot. *Microbiology Resource Announcements*, 1, e317–13.

Zhang, J., Shen, H., Pu, X., Lin, B. & Hu, J. (2014) Identification of *Dickeya zeae* as a causal agent of bacterial soft rot in banana in China. *Plant Disease*, 98, 436–442.

Zhang, X., Wu, D., Guo, T., Ran, T., Wang, W. & Xu, D. (2018) Differential roles for ArcA and ArcB homologues in swarming motility in *Serratia marcescens* FS14. *Antonie Van Leeuwenhoek International Journal of General and Molecular*, 111, 609–617.

Zhang, A., Han, Y., Huang, Y., Hu, X., Liu, P., Liu, X. et al. (2021) *vgrG* is separately transcribed from *hcp* in T6SS orphan clusters and is under the regulation of IHF and HapR. *Biochemical and Biophysical Research Communications*, 559, 15–20.

Zhou, J., Cheng, Y., Lv, M., Liao, L., Chen, Y., Gu, Y. et al. (2015) The complete genome sequence of *Dickeya zeae* EC1 reveals substantial divergence from other *Dickeya* strains and species. *BMC Genomics*, 16, 571.

Zhou, J., Zhang, H., Lv, M., Chen, Y., Liao, L., Cheng, Y. et al. (2016) SlyA regulates phytotoxin production and virulence in *Dickeya zeae* EC1. *Molecular Plant Pathology*, 17, 1398–1408.

SUPPORTING INFORMATION

Additional supporting information can be found online in the Supporting Information section at the end of this article.

How to cite this article: Chen, S., Hu, M., Hu, A., Xue, Y., Wang, S. & Liu, F. et al. (2022) The integration host factor regulates multiple virulence pathways in bacterial pathogen *Dickeya zeae* MS2. *Molecular Plant Pathology*, 23, 1487–1507. Available from: https://doi.org/10.1111/mpp.13244